LAPPEENRANTA UNIVERSITY OF TECHNOLOGY

FACULTY OF TECHNOLOGY

Master's Degree Programme in Technomathematics and Technical Physics

Polina Belova

MAGNETIC PROPERTIES OF $ZnGeP_2$:Mn

Examiners: Professor Erkki Lahderanta
PhD Alexander Lashkul

Supervisors: Professor Erkki Lahderanta
PhD Alexander Lashkul

ABSTRACT

LAPPEENRANTA UNIVERSITY OF TECHNOLOGY

FACULTY OF TECHNOLOGY

Master's Degree Programme in Technomathematics and Technical Physics

Polina Belova

Magnetic properties of $ZnGeP_2$:Mn.

Master's thesis

2009

73 pages, 62 figures and 1 table.

Examiners: Professor Erkki Lahderanta

PhD Alexander Lashkul

Keywords: $ZnGeP_2$:Mn, spintronics, magnetic measurements, magnetic properties.

In this work magnetic properties of $ZnGeP_2$:Mn were investigated in DC magnetic field with SQUID magnetometer in the temperature range from 3 K up to 400 K and in AC magnetic field with AC magnetometer in the temperature range from 77 K up to 350 K in frequency range from 500 Hz up to 18 KHz. Three $ZnGeP_2$:Mn samples were studied with Mn concentration c = 1.5 % mass, 3 % mass and 3.5 % mass.

ACKNOWLEDGEMENTS

This master's thesis was done in the Department of Mathematics and Physics at Lappeenranta University of Technology.

I am grateful to Professor Erkki Lahderanta for giving me opportunity to study at Lappeenranta University of Technology.

I would like to thank my supervisor PhD Alexander Lashkul for guiding me throughout the topic, his help, support, understanding and comments concerning this thesis.

I wish to express my gratitude to Yulia Shumeyko and Anastasia Grinenko.

My sincere appreciation goes to friends of mine from Punkkerikatu 5; it was really great time, thank you, guys.

Polina Belova

Lappeenranta, May 2009

TABLE OF SYMBOLS

Roman letters

p_m	magnetic moment
f	alternating magnetic field requency
H	magnetic field strength
M	magnetization
B	magnetic induction
T	absolute temperature
T_c	Curie temperature
T_N	Neel temperature
T_f	spin glass freezing temperature
V_{sig}	signal amplitude
w_r	signal frequency
q_{sig}	signal's phase
V	volume of the sample
c	concentration

Greek letters

χ	magnetic suspectibility
μ	magnetic permeability
χ'	real part of magnetic suspectibility
χ''	imaginary part of magnetic suspectibility
Θ	Curie temperature
Φ	magnetic flux

ACHRONYMS

AC	alternating current
DC	direct current
FC	field cooled
GPIB	general-purpose interface bus
PC	personal computer
TRM	thermoremanent magnetization
USB	universal serial bus
ZFC	zero field cooled
LED	light-emitting diode
PID	proportional, integral, derivative control
SQUID	superconducting quantum interference device
PSD	phase sensitive detector
AM	amplitude modulation
FM	frequency modulation
CMOS	complementary-symmetry metal-oxide semiconductor
SI	the international system of units
OPO	optical parametric oscillator

TABLE OF CONTENTS

1. Introduction

The basis of modern information technology is charge and spin of the electrons, however, charge properties of electrons are used in semiconductor materials (Si, GaAs), and spin properties are used in ferromagnetic materials. It is most prospective to use these properties in one material; in this case, magnetic properties can be changed by doping with magnetic impurities. All this is realized in a new class of materials – magnetic semiconductors. The most suitable are compounds like II-VI, III-V, II-IV-V_2. Use of ternary compounds instead of the binary ones allows to solve a problem of creation lasers, high LEDs, etc. by doping matrix crystals with rare-earth elements.

$ZnGeP_2$:Mn is one of the materials in which the room-temperature ferromagnetism is observed. The Curie temperature is about 310 K. The correlation of the transition temperature with the material composition can be obtained from temperature dependencies of magnetization. In this work such dependencies for $ZnGeP_2$:Mn with Mn concentration c = 1.5 % mass, 3 % mass and 3.5 % mass were investigated in AC and DC magnetic fields.

2. Magnetic properties of matter

All substances in nature when placed in a magnetic field change this field to some extent, and therefore they are called magnetic materials. In some materials (platinum, aluminum), which are called paramagnetics, the field slightly increases. In others, called diamagnetics (copper, bismuth) it slightly decreases; and in ferromagnetic materials (iron, nickel, cobalt) the field experiences a hundred, and sometimes even a thousand, times increase.

The physics quantity, which is equal to the ratio of the induction module B inside a homogeneous magnetic material to the magnetic induction vector module in vacuum B_0, created by the same source, is called the magnetic permeability of substance μ.

$$\mu = \frac{B}{B_0}. \qquad (1)$$

It is important to mention that Eq. (1) is strictly valid only for the homogeneous matters filling all space. In case of magnetic materials with finite sizes this ratio is applicable only when such magnetic material does not change the field structure (as in the example of a homogeneous core inside of a solenoid) [1, 2].

For the first time the idea that the magnetic phenomena in the long run are reduced to electric, was presented by Amper in 1825 when he stated the idea of the closed internal microcurrents circulating in each atom of a magnet. However, without any experimental confirmation of presence of such currents in a substance this theory “faded”. The electron was discovered by J. Thomson only in 1897 and the description of the atom’s structure was given by E. Rutherford and N. Bohr in 1913. In 1852 W. Weber came out with the assumption that each atom of a magnetic substance represents a tiny magnet, or a magnetic dipole, so full magnetization of a substance is reached when all separate nuclear magnets appear in a certain pattern (Fig. 1) [3].

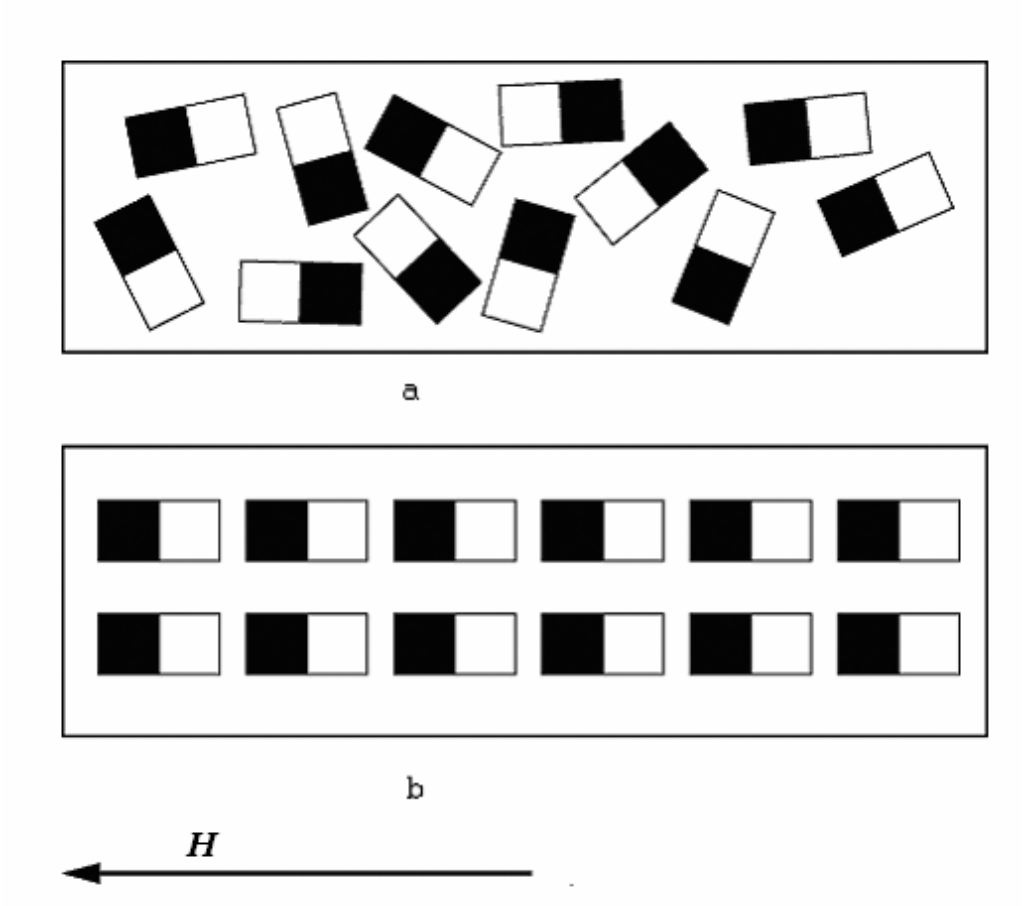

Figure 1. The early theory of magnetism: It was supposed that a substance is magnetized, when its separate atoms (each one of which is a small magnet), in the absence of field, are located chaotically (a), but under the influence of an external field they settle in a certain pattern (b).

The approach to the problem proposed once by Amper, reincarnated in 1905 when P. Langevin explained the behavior of paramagnetic materials, having attributed an internal non-compensated electronic current to each atom. According to Langevin, these currents form tiny magnets that are chaotically oriented, when the external field is absent, but get an ordered orientation after its application. In this case the approach towards full order corresponds to the magnetization saturation. Additionally, Langevin introduced a concept that the magnetic moment for a separate magnet equals the product of "a magnetic charge" poles by the distance between those poles. Thus, weak magnetism of

paramagnetic materials is caused by the total magnetic moment created by non-compensated electronic currents.

In 1907 P. Weiss introduced the concept of "domain", which became a very important contribution to the modern theory of magnetism. Weiss represented domains in the form of small "colonies" of atoms, inside which the magnetic moments of all atoms, for some reason, are forced to keep an identical orientation, so that each domain is magnetized to the level of saturation. A separate domain might have a linear size of approximately 0.01 mm, and accordingly the volume of 10^{-6} mm^3 [3, 4].

Magnetic properties of materials are defined by magnetic properties of atoms or elementary particles (electrons, protons and neutrons), that form an atom. It is now established that magnetic properties of protons and neutrons are almost 1000 times weaker than magnetic properties of electrons. Therefore, magnetic properties of a substance are generally defined by the electrons that form the atom.

One of the major properties of the electron is its possession of not only an electric, but also of its own magnetic field. The magnetic field that the electron possesses is called **spin**. The electron creates a magnetic field also using the orbital movement around the nucleus, which can be connected with a circular microcurrent. Spin fields of electrons and the magnetic fields caused by their orbital movements define wide spectrum of magnetic properties of materials.

2.1. Diamagnetism and paramagnetism

Substances vary by their magnetic properties. In majority of substances these properties are expressed poorly. Weak-magnetic substances are divided in two big groups – paramagnetics and diamagnetics.

Diamagnetism persists only while an external field is applied. Diamagnetic materials get magnetized in direction opposite to an applied magnetic field. When the external field is absent, the atoms of diamagnetic materials have their own magnetic fields defined by electrons and also by their orbital movement.

These fields are completely compensated. The relative permeability μ_r is less than unity, and the magnetic susceptibility χ_m is negative.

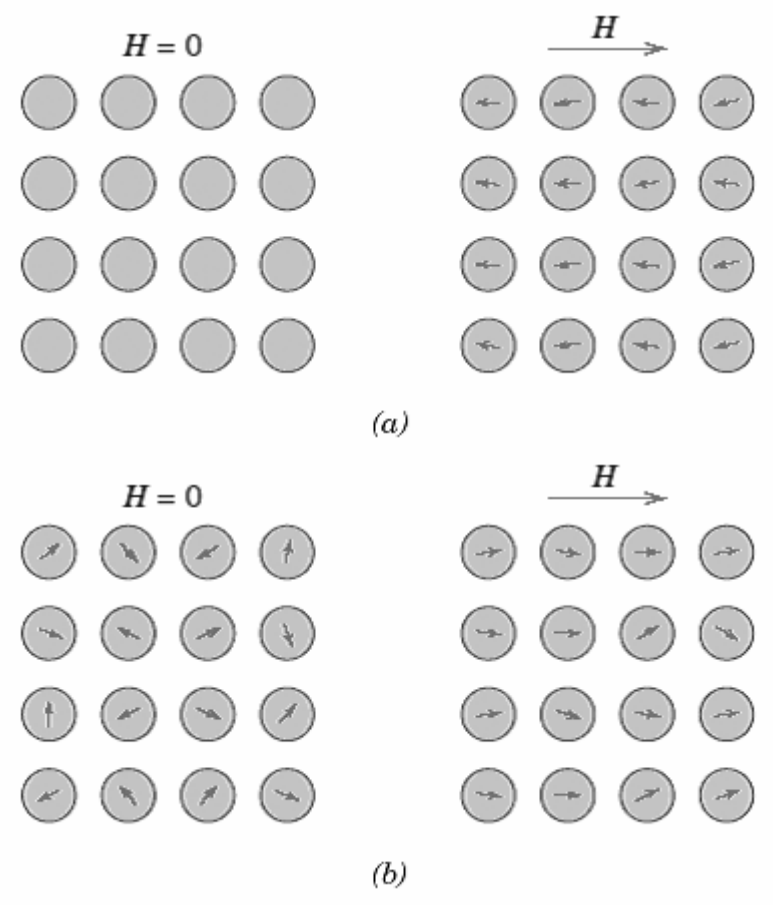

Figure 2. (*a*) The atomic dipole configuration for a diamagnetic material with and without magnetic field. In the absence of an external field, no dipoles exist; in the presence of a field, dipoles are induced and then are aligned opposite to the field direction. (*b*) Atomic dipole configuration with and without an external magnetic field for a paramagnetic material [5].

Table 1 presents the susceptibilities of several diamagnetic materials. Note that atoms of any substances have diamagnetic properties. However, in many cases diamagnetism of atoms is masked by stronger paramagnetic effect. The diamagnetism phenomenon has been opened by M. Faraday (1845).

Paramagnetic materials are magnetized in an external magnetic field in a direction of the field. This property of materials is called paramagnetism (Fig. 2 b). In a non-homogeneous magnetic field paramagnetics are drawn into the area of a strong magnetic field. Their magnetic susceptibility is always positive. Paramagnetism is characteristic for materials, which atoms, ions or molecules have their own magnetic moments, but in the absence of an external field these moments are oriented chaotically and bulk magnetization of substance is absent. The magnetic moments can be caused due to the orbital movement of the electrons in the clusters of atoms or molecules (orbital paramagnetism), or the spin moments of the electrons (spin paramagnetism), the magnetic moments of an atom nucleus (nuclear paramagnetism) [6, 7].

Susceptibilities for paramagnetic materials are in range 10^{-5} - 10^{-2} (Table 1). A schematic *B(H)* curve for a paramagnetic material is also shown in Fig. 3.

Both diamagnetic and paramagnetic materials are considered to be nonmagnetic because they exhibit magnetization only in the presence of an external field. Also, for both, the flux density *B* within them is almost the same as it would be in a vacuum.

Table 1. Room-temperature magnetic susceptibilities for diamagnetic and paramagnetic materials [5].

Diamagnetic materials		Paramagnetic materials	
Material	Susceptibility χ_m(volume) (SI units)	Material	Susceptibility χ_m(volume) (SI units)
Aluminum oxide	$-1.81 \cdot 10^{-5}$	Aluminum	$2.07 \cdot 10^{-5}$
Copper	$-0.96 \cdot 10^{-5}$	Chromium	$3.13 \cdot 10^{-5}$

Gold	$-3.44 \cdot 10^{-5}$	Chromium chloride	$1.51 \cdot 10^{-5}$
Mercury	$-2.85 \cdot 10^{-5}$	Manganese sulfate	$3.70 \cdot 10^{-5}$
Silicon	$-0.41 \cdot 10^{-5}$	Molybdenum	$1.19 \cdot 10^{-5}$
Silver	$-2.38 \cdot 10^{-5}$	Sodium	$8.48 \cdot 10^{-5}$
Sodium chloride	$-1.41 \cdot 10^{-5}$	Titanium	$1.81 \cdot 10^{-5}$
Zinc	$-1.56 \cdot 10^{-5}$	Zirconium	$1.09 \cdot 10^{-5}$

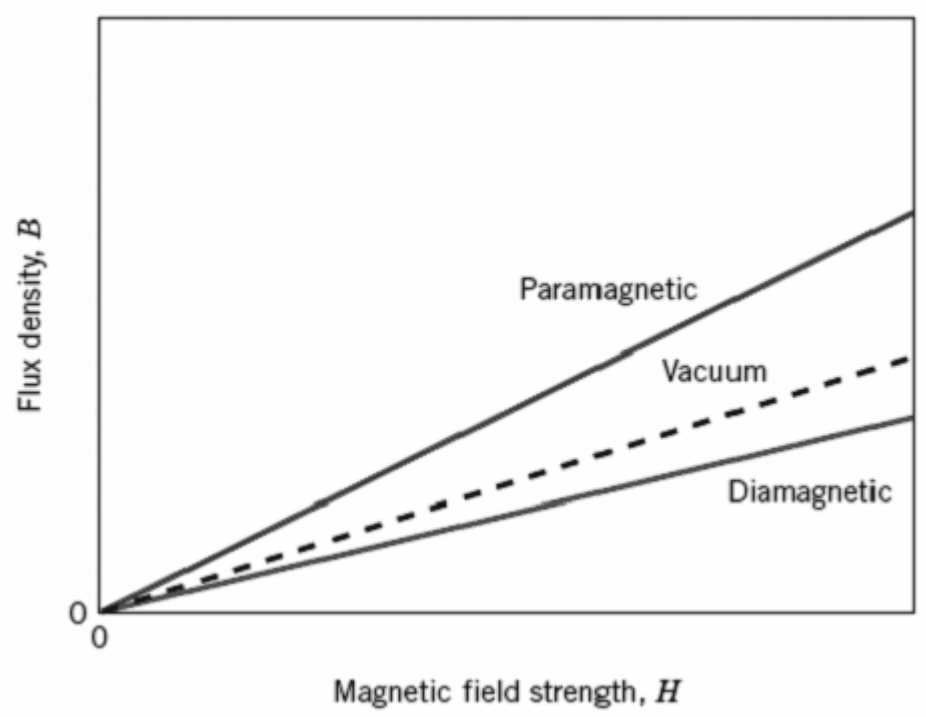

Figure 3. Schematic representation of the flux density *B* versus the magnetic field strength *H* for diamagnetic and paramagnetic materials [5].

2.2. Ferromagnetism

Ferromagnetism is a magnetically ordered state of materials, in which the majority of the magnetic moments of atoms are parallel to each other, so the material possesses spontaneous magnetization.

Materials, in which occurs a ferromagnetic ordering of the magnetic moments, are called ferromagnetics (Fig. 4). Crystals of transition metals (iron, cobalt, nickel), of some rare-earth elements and of some alloys, ferrites, and also some metal glasses are examples of the ferromagnetic materials.

The main property of ferromagnetic is the ability to remain magnetized after the external magnetic field is removed. At high temperatures ferromagnetics get demagnetized and turn into paramagnetics. The temperature at which ferromagnetic behavior disappears is called the Curie point, T_c, (for iron this temperature is equal to 770 ºC, for cobalt 1130 ºC). In spite of the fact that not many ferromagnetics exist in nature, they have a high practical value, and not only because of a considerable magnetic field amplification (up to ten thousand times), but also because of their specific property, residual magnetization, thanks to which all constant magnets exist and many systems of record and storing of information have been created [7, 8].

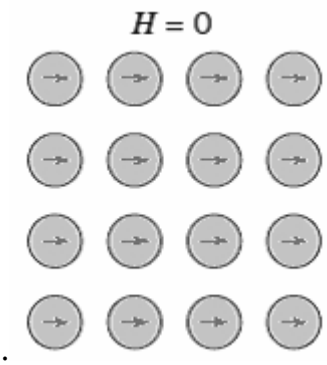

Figure 4. Schematic illustration of the mutual alignment of atomic dipoles for a ferromagnetic material, which will exist even in the absence of an external magnetic field [5].

2.3. Antiferromagnetism and ferrimagnetism

2.3.1. Antiferromagnetism

Antiferromagnetism is a magnetically ordered state of crystal substance, in which the magnetic moments of atoms (ions) in the neighboring lattice points are focused so (as a rule, antiparallel) that bulk magnetization of substance is equal to zero. Under the influence of an external magnetic field antiferromagnetics get weak magnetization. In Neel temperature, T_N, the magnetization is lost and transition to a paramagnetic condition takes place.

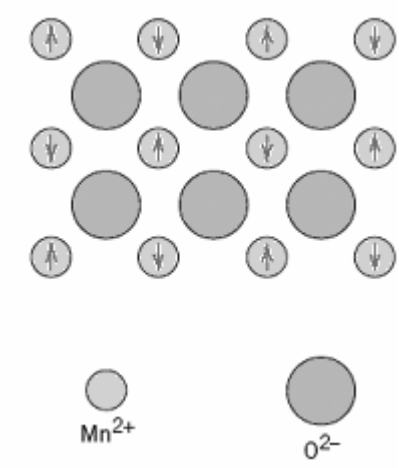

Figure 5. Schematic representation of antiparallel alignment of spin magnetic moments for antiferromagnetic manganese oxide [5].

2.3.2. Ferrimagnetism

A material is said to exhibit ferrimagnetic order when, first, all moments on a given sublattice are pointed in a single direction and, second, the resulting moments of the sublattices lie parallel or antiparallel to one another [5]. Ferrimagnetism disappears above the Curie temperature (T_c).

2.4. Spin glasses

Among many types of the magnetic-ordered materials [9] a special place belongs to so-called spin glasses. Orientation of the elementary magnetic moments of spin glass atoms or clusters in temperatures below some value T_f has no spatial periodicity. It randomly varies in space, just like in the case of atoms that are casually located in usual glass. Unlike paramagnetics, where elementary magnetic moments fluctuate in time, spin glasses are characterized below certain temperature by the presence of "frozen" magnetic moments. That is, the atom magnetic moments have nonzero average vector values in terms of time [10, 11]. The latter is confirmed by Mössbauer measurements, which demonstrate the presence of effective magnetic fields that influence magnetic atoms. As investigations show, the universal reason of occurrence of the spin glass condition is a combination of nuclear disorder and a competition of exchange interactions. Hence, study of a spin glass condition is part of the general problem of studying of atomic-disorder magnetics, that is, substances, in which the nuclear disorder is a consequence of random atomic distribution of various types (the chemical disorder) or a disordered distribution in atomic space of one type (vitreous or an amorphous condition).

An ideal spatial order is observed in a perfect crystal. It represents a set of a big number of identical atoms or molecules, packed in a regular way in the volume of a crystal.

The elementary type of the disorder is realized in a substitutional solid solution. In an ideal crystal it is possible to replace an atom of an element *A* with an atom of other element *B* without essential lattice distortion. If in this case, lattice points, where the replacement of atoms *A* with atoms *B* occurs, do not form a regular lattice, we have an example of a disorder of replacement. Otherwise, a so-called superlattice is created.

Another type of a disordered system is materials, in which the atoms distribution does not correspond with the lattice. Amorphous materials and liquids are examples of this type.

Frustrated are called couplings, those connect the magnetic moments, in which mutual orientation does not correspond with a sign on their exchange couplings.

The presence of frustrated couplings is the main characteristic of disordered magnetic system. It leads to splitting the basic condition into a very big, exponentially growing with an increase in the number of magnetic atoms in the system number of underlying (in terms of energy) conditions.

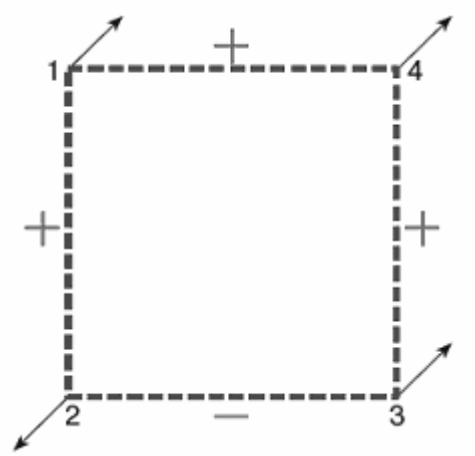

Figure 6. Frustrated square. By signs + and are shown ferromagnetic and antiferromagnetic exchange coupling, correspondingly [10]. Magnetic moment in corner 2 can not fulfill all interactions.

2.4.1. Properties of spin glasses

*Magnetic susceptibility***:**

Distinctive feature of spin glass behavior is the presence of a sharp hump on the temperature dependence of a magnetic susceptibility $\chi(T)$, measured in small magnetic fields and low frequencies (approximately hundred hertz). In Fig. 7, such dependence for an AuFe alloy is shown [12]. It is visible that the temperature T_f, when this hump is observed, increases with an increase of iron concentration in the alloy. Another important feature of susceptibility behavior is its strong dependence on magnetic field strength in which it is measured.

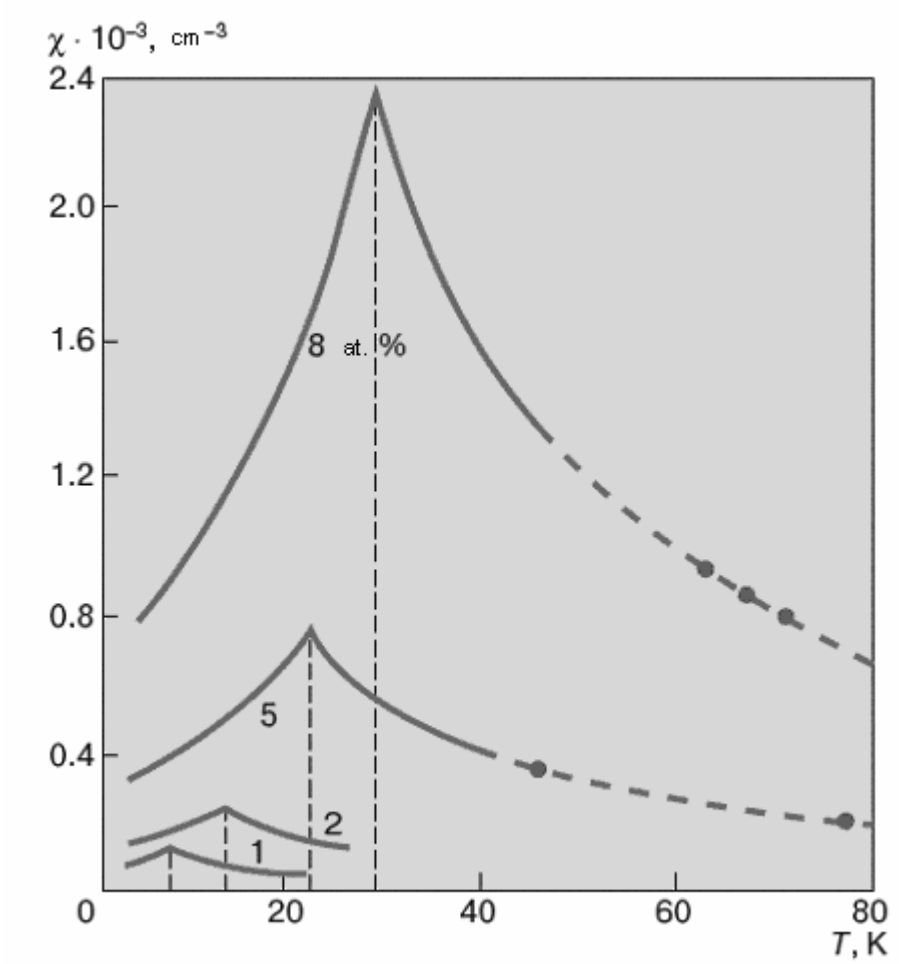

Figure 7. Lowfield magnetic susceptibility *χ(T)* of AuFe alloys with the iron concentration 1, 2, 5 and 8 at. % [12].

Magnetization:

It is characteristic for spin glasses that magnetic moment, induced in the spin glass by external magnetic field, depends not only on the field value, but also on the history of the sample.

Let's consider the elementary model of spin glass, so-called Ising model of Sherrington-Kirkpatrick [13, 14]. Energy of magnetic system of spin glass in this model follows Eq. 2:

$$H = -\sum_{i,j} J_{ij}\sigma_i\sigma_j, \qquad (2)$$

where i, j are numbers of the magnetic moments of the atoms, $\sigma = \pm 1$, parameters of exchange interaction are assumed independent from the distance between interacting atoms, and their values are distributed with Gaussian law,

$$\rho(J_{ij}) = (2\pi J)^{-1/2} \exp\left[-\frac{(J_{ij} - J_0)^2}{2J^2}\right]. \qquad (3)$$

Distribution parameters, dispersion of J and its average value J_0, depend on the number of magnetic atoms in system N:

$$J_0 = \frac{K_0}{N}, \qquad J = \frac{K}{N^{1/2}}. \qquad (4)$$

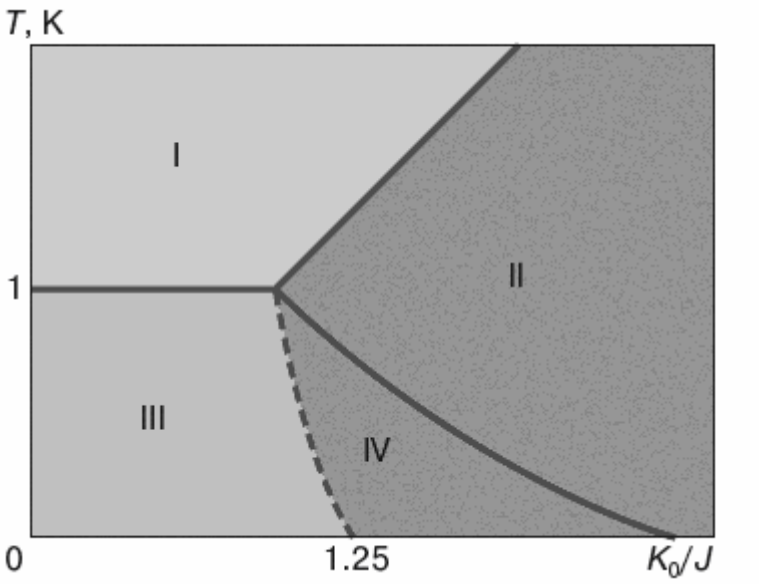

Figure 8. Magnetic phase diagram of spin glass in Sherrington-Kirkpatrick model: I is paramagnetic phase, II, IV are ferromagnetic phases, III is spin glass phase [13].

Based on the analysis of this model, D. Sherrington and S. Kirkpatrick obtained magnetic phase diagram (Fig. 8) on a plane (temperature-parameter K_0). In area number III is the spin glass phase, for which the Edwards-Anderson's parameter is not zero. The total magnetic moment of the system in this phase is equal to zero. Susceptibility and thermal capacity have a hump on a straight line dividing a paramagnetic phase I where the Edwards-Anderson's parameter is equal to zero, and a phase of spin glass III.

3. Spintronics

Spintronics or electronics, that uses spin-related phenomena, attracted a lot of attention because of its potential applicability for new functional devices, which combine charge and magnetic properties of the electron [15].

Spintronics is a field of science that studies interaction of the magnetic moments of electrons (spins) with electromagnetic fields and develops spin-electronic devices and equipment, based on discovered phenomena and effects.

According to the theory of magnetism, it is considered that electron has quantum property, spin, because of which it behaves like an arrow of a compass, rotating around the axis and connecting its (the electron's) southern and northern poles. Spins of the electron can be oriented in the directions, that are usually called "spin-upwards" (major spin) and "spin-downwards" (minor spin) (Fig. 9).

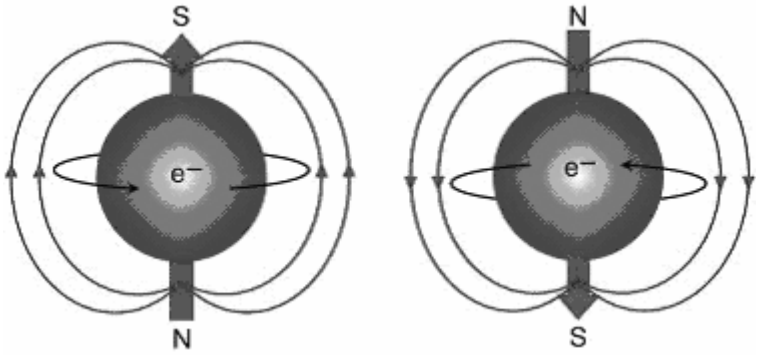

Figure 9. "Spin-upwards" (major spin) and "spin-downwards" (minor spin).

If one places the electrons in a magnetic field, their spins will be aligned along the field direction. In this case they will precess around the field lines. One can compare this phenomenon to the orbital precession of our planet.

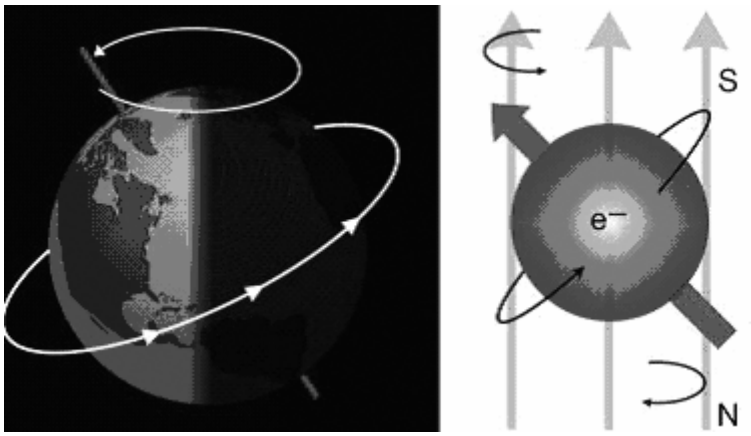

Figure 10. The orbital precession of our planet and electron.

If the field is switched off, spin precession is terminated and its orientation is fixed. In other words, using precess effect, it is possible to change a spin condition of the electrons, and by doing that, to change the bit of the information, transferred by electrons, from logic "0" to "1" and back.

Spintronics is used to manufacture devices that use the creation of nonequilibrium spin density in the semiconductor, the driving of spin orientation by external fields and detecting a formed spin condition [16].

4. Magnetic properties of $ZnGeP_2$

$ZnGeP_2$ is II-IV-V_2 chalcopyrite crystal with a band gap 2.0 eV at 300 K [17]. It is a tetrahedrally bonded ternary compound with a c/a ratio equal 1.96, which crystallizes in a form "genealogically" related to the zinc-blende crystal structure. It is gaining importance as a nonlinear optical material. $ZnGeP_2$ has good transparency in the range of 0.7 - 12 μm [18]. It is currently the most promising optical material for nonlinear optical devices such as tunable mid-infrared optical parametric oscillator (OPO) laser systems [19].

Energy band structure of $ZnGeP_2$ is presented in Fig. 11.

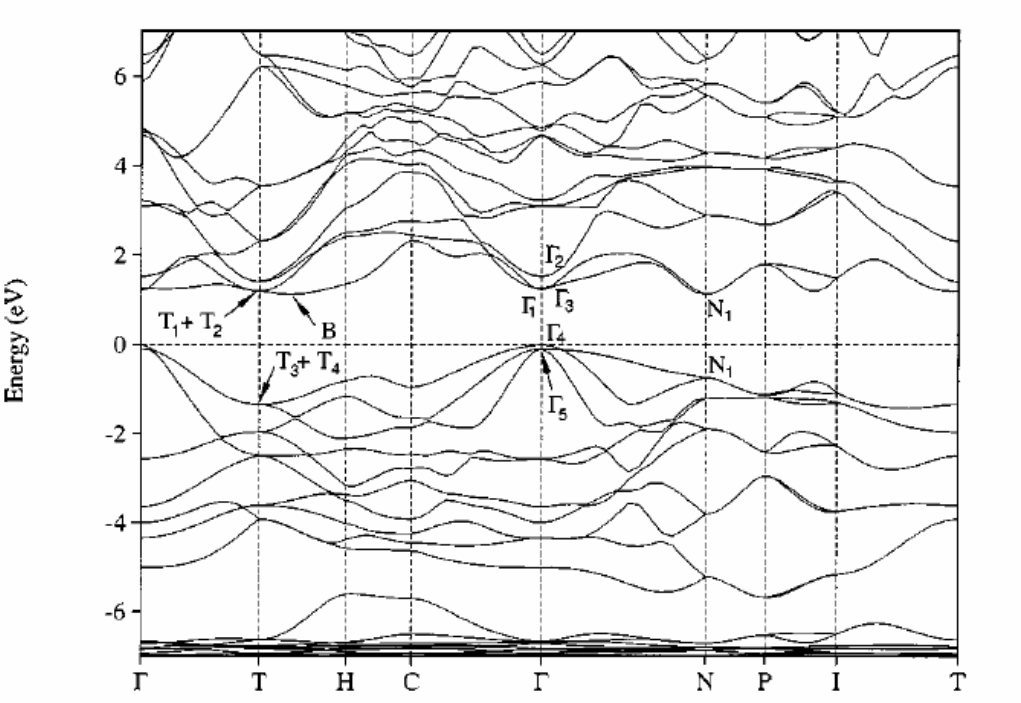

Figure 11. Energy band structure of $ZnGeP_2$ in the local-density approximation [20].

To prepare of single crystals and polycrystals of $(Zn_{1-x}Mn_x)GeP_2$ was used high-purity (99.999%) zinc (Zn), germanium (Ge), manganese phosphide (Mn_3P_2), and phosphorus (P) powders as starting materials with particle size < 200 mesh.

To grow crystals, the Bridgman-Stolberg method was used. A method of growing single crystal ingots or boules in the temperature gradient is the Bridgman technique. It is popular method to produce certain semiconductor crystals, such as II-V crystals, gallium arsenide, (ZnSe, CdS, CdTe), II-IV-V_2 system. The method involves heating polycrystalline material in a container above its melting point and slowly cooling it starting from one end where a seed crystal is located. Single crystal material is formed along the container. The process can be carried out in a horizontal or vertical geometry [21].

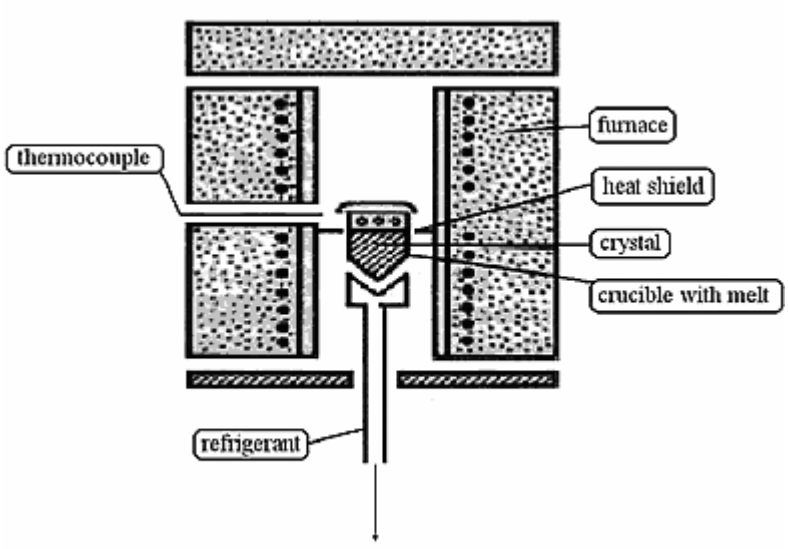

Figure 12. Bridgman-Stolberg method [21].

Chalcopyrite crystal structure is presented in Fig. 13. It is the zinc-blende superlattice structure with specific ordered arrangement of the Zn and Ge cations accompanied by small structural distortions. It can be described as a body-centered tetragonal primitive unit cell. The lattice vectors, $\mathbf{a}_1 = (-a/2, a/2, c/2)$, $\mathbf{a}_2 = (a/2, -a/2, c/2)$, and $\mathbf{a}_3 = (a/2, a/2, c/2)$ are indicated in Fig. 13. The structural parameters are the c/a ratio, the a lattice constant and the internal structural parameter u, which determines the position of the anion in its nearest neighbor tetrahedron. For example, the atom in the left lower corner has

coordinates ($a/4$, ua, $c/8$). In the ideal structure the structural parameters are $c/a = 2$ and $u = 1/4$ [20].

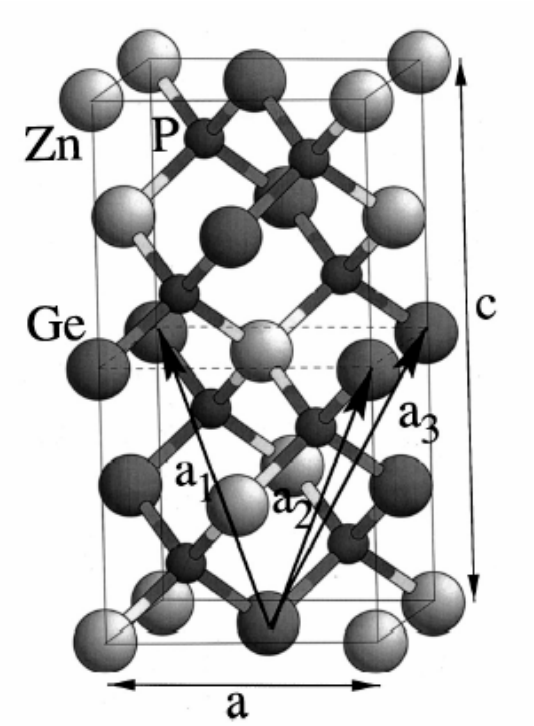

Figure 13. Crystal structure of chalcopyrite [20].

5. Magnetic measurements

Magnetization of material in magnetic field means, that because of molecular currents any physically small volume of material in magnetic field gets the magnetic moment. Hence, external sources, as well as the internal currents that circulate within atoms and molecules, participate in the creating of magnetic field in material [22].

Therefore, material in magnetic field $\vec{B}_0$ becomes a source for magnetic field $\vec{B}'$ which is imposed on the field $\vec{B}_0$. Induction vector of resulting magnetic field is

$$\vec{B} = \vec{B}_0 + \vec{B}'. \tag{5}$$

Magnetization of the magnetic material is characterized by the magnetic moment of the unit volume. Generally, when magnetic material is magnetized non-uniformly, the magnetization in the given point is equal to

$$\vec{M} = \frac{\sum \vec{P}_m}{\Delta V}, \tag{6}$$

where $\vec{P}_m$ is magnetic moment of the single molecule. Here ΔV is infinite small volume in a vicinity of the chosen point. Magnetization M is connected not with a magnetic induction, but with magnetic field strength H:

$$\vec{M} = \chi H, \tag{7}$$

where χ is magnetic susceptibility.

Magnetic field strength is an auxiliary value, which is introduced for the account of the magnetic field, created only by currents that flow along the conductors.

Objectives of magnetic measurements

With the help of methods and equipment of magnetic measurements, various problems can be solved nowadays [23]. The basic measurements are:

- measurement of the magnetic values (magnetic induction, magnetic flux, magnetic moment, etc.);

- studying characteristics of magnetic materials;

- investigations of electromagnetic mechanisms;

- measurement of the Earth magnetic field and the fields of other planets;
- study of physical and chemical properties of materials (the magnetic analysis);

- investigation of magnetic properties of atom and an atomic nucleus;

- definition of defects in materials and products (magnetic flaw detection, etc.) [24].

Despite of variety of the problems, solved by magnetic measurements, some basic magnetic values are defined: magnetic flux Φ, magnetic induction B, magnetic field strength H, magnetization M, magnetic moment, etc.

It is important to note, that in many types of magnetic measurement, the value that is actually measured is not magnetic one but an electric one. This electric value is transformed from the magnetic value during measurement [25].

The magnetic value is defined by calculation, based on the identified dependences between magnetic and electric values.

Theoretical basis of similar methods is the second Maxwell equation, which connects a magnetic field and an electric field; these fields display special kind of matter called an electromagnetic field.

Other, not only electric, magnetic field displays are also used in magnetic measurements, the examples of such displays are mechanical, optical.

During the measurements of magnetic moment or magnetic susceptibility in a constant magnetic field, the magnetic moments try to orient parallel to the applied field.

Magnetization is measured in various values of the applied field H_{dc}. If the sample is placed in an alternating magnetic field, the magnetic moments of the sample change orientation periodically in accordance with the field. SQUID is used for conducting the measurements in a constant magnetic field.

The most sensitive device available for measuring magnetic fields is SQUID (Superconducting Quantum Interference Device). SQUID in the MPMS (Magnetic Property Measurement System) is the source of the instrument's remarkable sensitivity. It does not directly detect the magnetic field from the sample. The detection coil is a superconducting three coils, configured as a second-order gradiometer. The measurement principle is: moving a sample through the superconducting detection coils, which are located outside the sample chamber and in the magnet center. If the sample moves through the coils, the magnetic moment of the sample induces an electric current in the detection coils. Any change of magnetic flux in the detection coils produces a change in the current of the detection circuit, which is proportional to the change in the magnetic flux. The superconducting connecting wires, the superconducting detection coils, and the SQUID superconducting input coil form one closed superconducting loop, which is illustrated in Fig. 14. The SQUID is working as a highly sensitive current-to-voltage convector. Because of that, the variations in the current in the detection coils produce corresponding variations in the SQUID output voltage. These variations are proportional to the magnetic moment of the sample. In a calibrated system, variations of voltage are measured from the SQUID detector output when sample is moving through the detection coils. This provides highly accurate measurement of the sample's magnetic moment. Using a piece of metal having known mass and known magnetic susceptibility the system can be accurately calibrated. The gradiometer configuration is used to reduce noise, caused by fluctuations in the large magnetic field of the superconducting magnet, in the detection circuit, and minimize background drifts in the SQUID detection system [26].

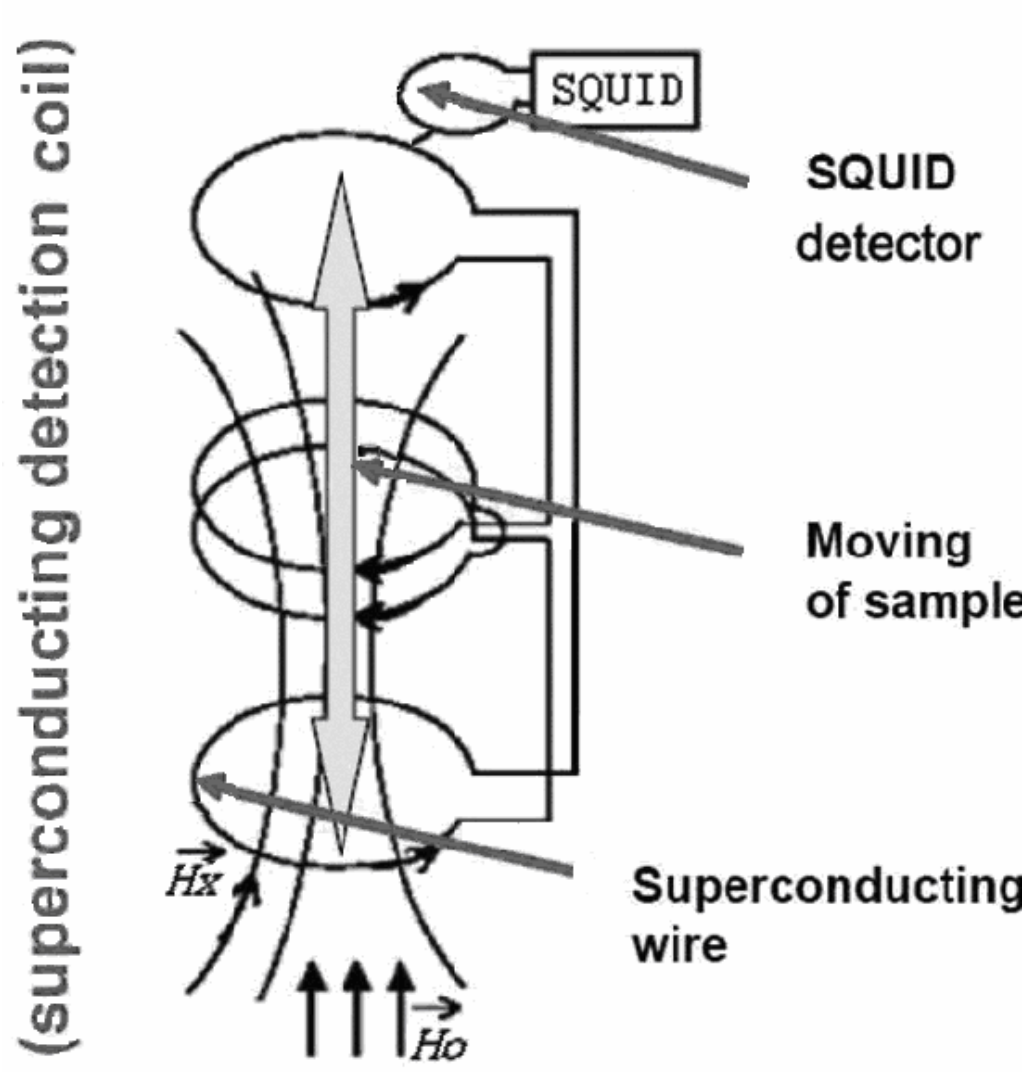

Figure 14. SQUID, configuration [26].

For the measurement of magnetic susceptibility in an alternative field (AC), a AC-susceptometer is used. Its design is based on the principle of co-axial mutual inductance technique. AC susceptometer consists of the primary coil, which generates an AC magnetic field, and two secondary oppositely wound coils, which form the basic measuring unit. The voltage measured over these two detection coils is ideally zero, when a sample is absent. If one inserts a sample centered in one of the secondary coils, the AC voltage will be directly proportional to the amplitude of AC susceptibility $\chi = \chi' - i\chi''$ [27].

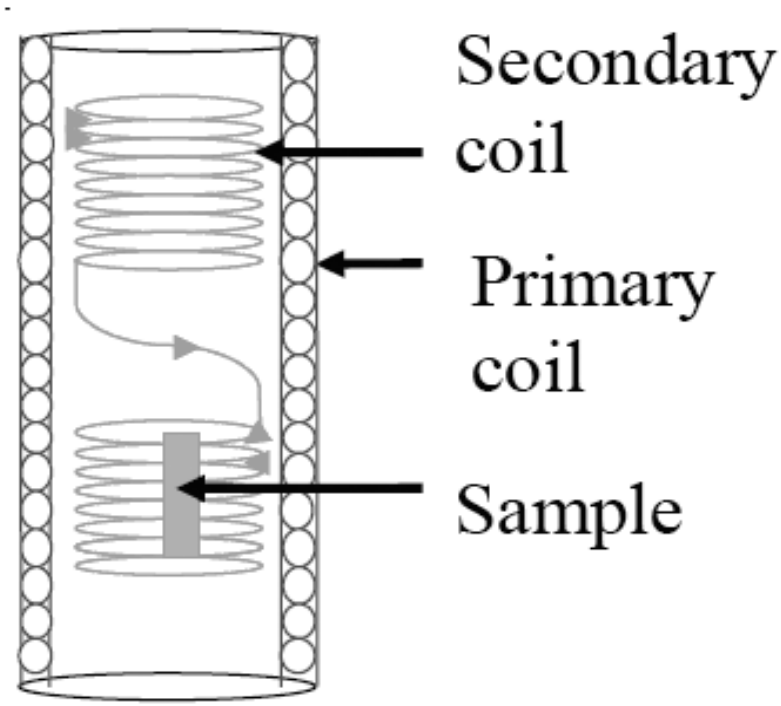

Figure 15. Detecting system of AC susceptometer [27].

6. Experimental facility

6.1. SQUID

DC magnetization of samples was measured with Cryogenic S600 SQUID magnetometer shown in Figs. 16 - 17.

Figure 16. A Cryogenic S600 SQUID magnetometer.

Using a Quantum Design Superconducting Quantum Interference Device (SQUID) magnetometer (Fig. 17), the magnetization of $ZnGeP_2$:Mn single crystals was measured in the temperature range of 5 - 400 K and in magnetic fields up to 5 T. A Cryogenic system is completed with automatized instrument control, data acquisition and analysis using the National Instrument's LabVIEW software.

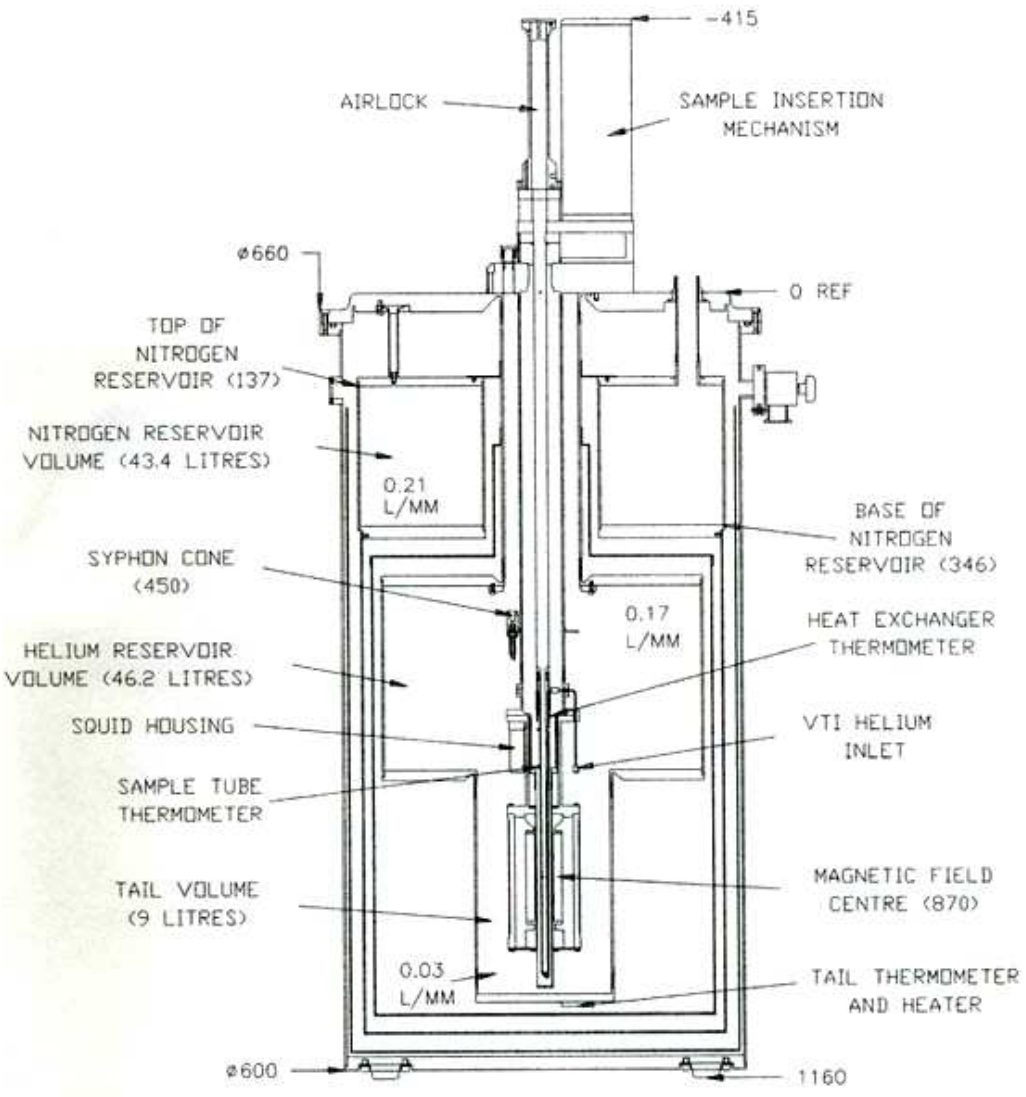

Figure 17. Schematic of SQUID cryostat [28].

Magnetic flux from the magnetic moment of the sample was detected by the SQUID device, because the sample was moved through the SQUID coils. The upper and lower coils of the SQUID circuit are similar sequentially connected, and wound in the opposite directions (Fig. 18). The flux resulting from the applied field and any stray fields, which are constant along *z*, is compensated. When the sample is moved through the coils compensation current in superconducting circuit produces the magnetic flux in the SQUID. The amplitude of the current required for compensation is proportional to the

magnetic moment of the sample. *m* is known as the total magnetic moment of the sample and it is measured in absolute units of $A \cdot m^2$ (SI) or *emu*. Electromagnetic unit, *emu*, is the CGS unit for moment; the CGS unit for magnetic field is Gauss.

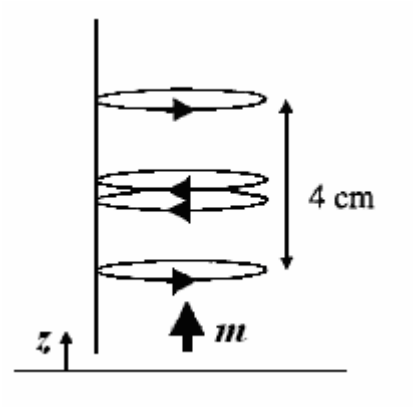

Figure 18. Schematic of the secondary coil.

Magnetization is $M = \frac{\mu}{V}$, where *V* is volume of the sample is measured in a magnetometer. Magnetic susceptibility defined as *dM/dH*, when $H \rightarrow 0$, is constant in magnetic field so that $\chi = M/H$ in linear materials. χ is unitless, because SQUID measures the magnetic moment in *emu* (1 *emu* = 1 erg/Gauss).

It is more usual to normalized the magnetic moment to the mass or molar mass of the sample than to the sample volume. The susceptibility is therefore presented in units of cm^3/g or cm^3/mole of material [29].

6.2. AC magnetometer

AC magnetometer measures susceptibility and magnetization of the sample in the temperature range 77 K - 350 K in AC magnetic field. Control is done by PC with LabVIEW software.

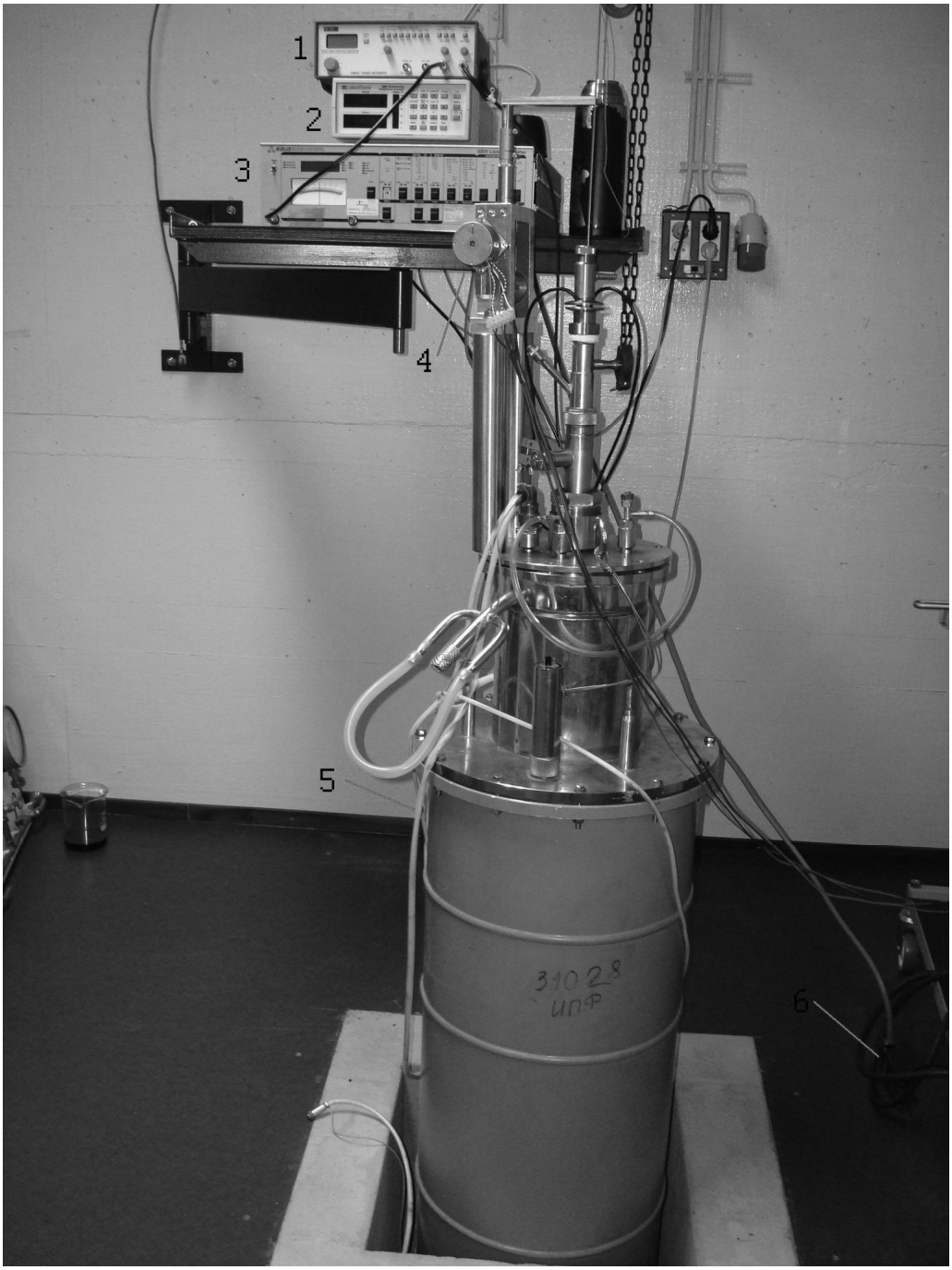

Figure 19. AC magnetometer. 1 is AC generator, 2 is temperature controller, 3 is lock-in amplifier, 4 is stepper motor, 5 is cryostat, and 6 is IEEE 488.1 interface (GPIB).

AC magnetometer consists of AC generator, lock-in amplifier, temperature controller, stepper motor, sample holder and cryostat.

The cryostat was cooled by liquid nitrogen.

Inside the cryostat 2 tubes exist: external and auxiliary. On the auxiliary tube the sample holder and heater are located. The heater is prepared as a coil of resistive wire and is located far enough from the sample not to effect measurements. Sample is fixed by teflon type on the holder, which is made of aluminum strips that have been stuck together by glue. The sample possesses good heat conductivity and is located between of the copper-constantan thermocouples, which are fixed on distances of 24 mm and 102 mm from the end of the sample holder. The temperature of the sample is defined as arithmetic average value of the thermocouples indications.

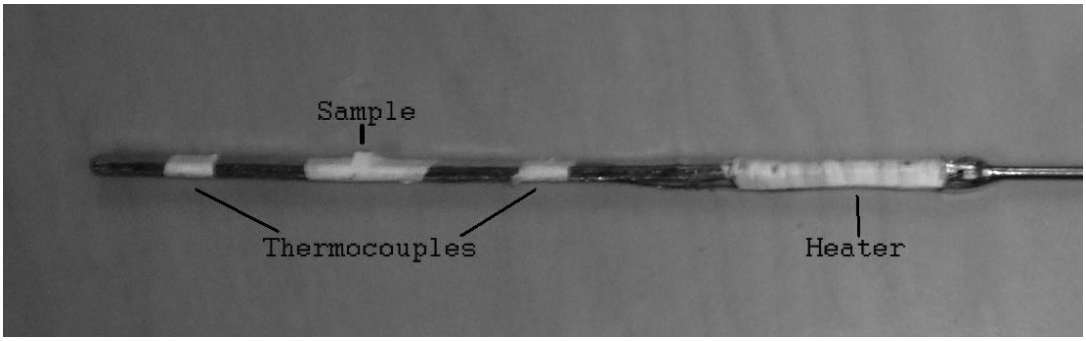

Figure 20. Auxiliary tube, sample holder and heater.

On the opposite end of the auxiliary tube is fixed connectors of heater and thermocouples to the temperature controller. During the experiment, the auxiliary tube moves inside the external tube which has bigger diameter. On an external tube secondary thermocouples, and also cables for the synchronous amplifier and the alternating voltage generator exist.

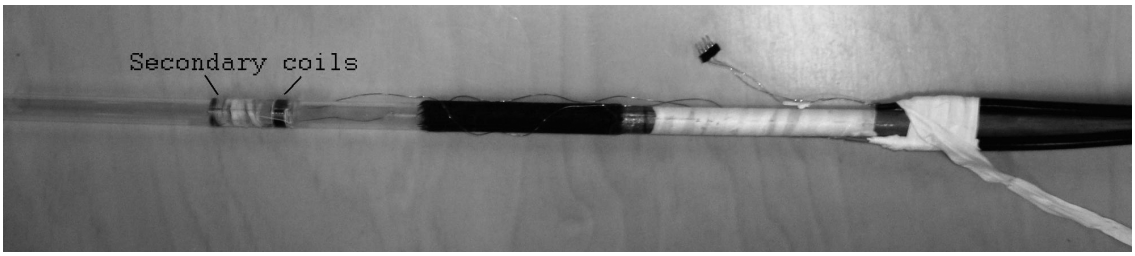

Figure 21. External tube. Secondary coils.

Primary coil is wound on a plastic tube which is fixed by bolts on the external tube.

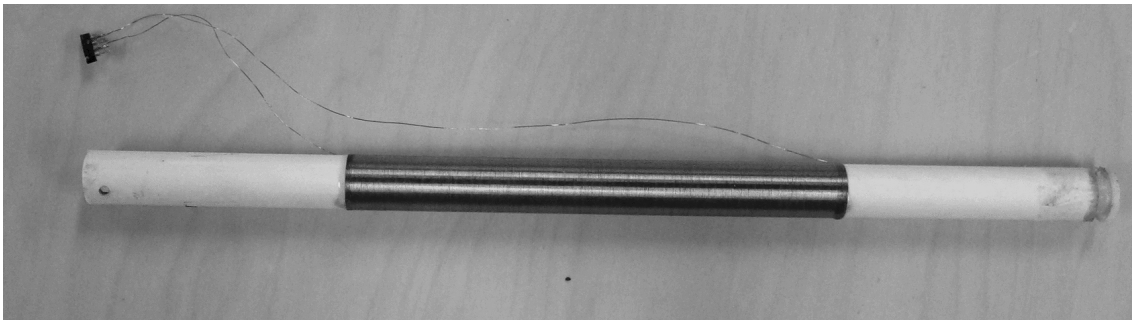

Figure 22. Primary coil.

The installation scheme:

Lock-in amplifier takes the signal from the secondary coil and is connected with the AC generator, which feeds the primary coil. PC controls and takes signals from the temperature controller and lock-in amplifier, and also gives the signal and feeds the stepper motor.

Before the measurements it is necessary to set manually the frequency and the signal amplitude on the AC generator. After that, the measurement temperature values are set to the program. When the program is started, the temperature is stabilized by the temperature controller, according to the set points and the

temperature stabilization is awaited with the set error. When it happens, the program saves the data from the lock-in amplifier and sends the signal to the step motor, which moves the sample through the coils with a certain velocity and amplitude.

6.2.1. **Lock-in amplifier**

One of the main parts of AC magnetometer is a lock-in amplifier (5205 model by EG&G), which is shown in the Fig. 23. IEEE 488.1 interface (GPIB) is used to connect lock-in amplifier and PC. The GPIB Controller for Hi-Speed USB is presented in Fig. 24.

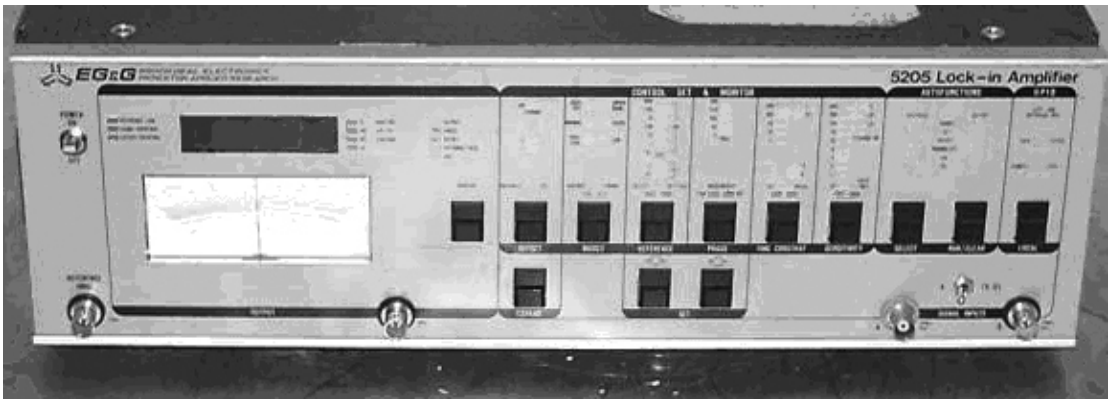

Figure 23. Lock-in amplifier (model 5205 by EG&G), front panel.

Figure 24. GPIB Controller for Hi-Speed USB [30].

A lock-in amplifier provides a DC output directly proportional to the AC signal [31]. A phase sensitive detector (PSD), which does the conversion and is known as a demodulator or mixer, is the basic part of the lock-in amplifier. This is essentially a multiplier, analog or digital. The scheme of a typical lock-in amplifier is presented in Fig. 25.

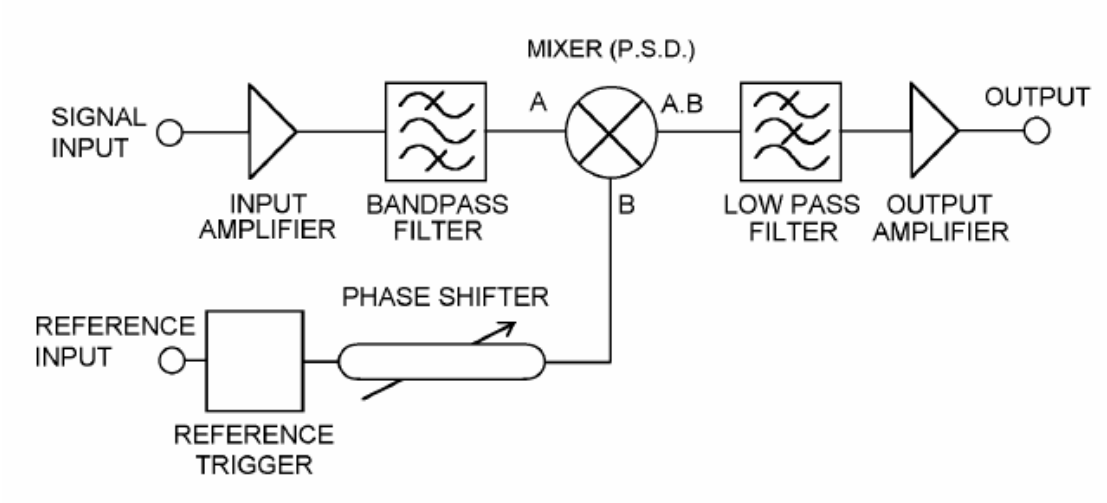

Figure 25. The block diagram of a typical lock-in amplifier [31].

Detector multiplies two signals together, and the following analysis shows how this gives the required outputs.

Measurements of lock-in amplifiers require a frequency reference. From function generator and the lock-in defines the response from the experiment at the reference frequency.

A square wave at frequency w_r is the reference signal (Fig. 26). If the sine output from the function generator is used to start the experiment, the response might be the signal waveform

$$V_{sig}\sin(\omega_r t + q_{sig}), \qquad (8)$$

where V_{sig} is the signal amplitude, ω_r is the signal frequency, and q_{sig} is the signal's phase.

Lock-in generates its own internal reference signal, usually by a phase-locked-loop locked to the external reference. In Fig. 26 the external reference, the lock-in's reference and the signal are shown. The internal reference is

$$V_L \sin(\omega_L t + \Theta_{ref}). \tag{9}$$

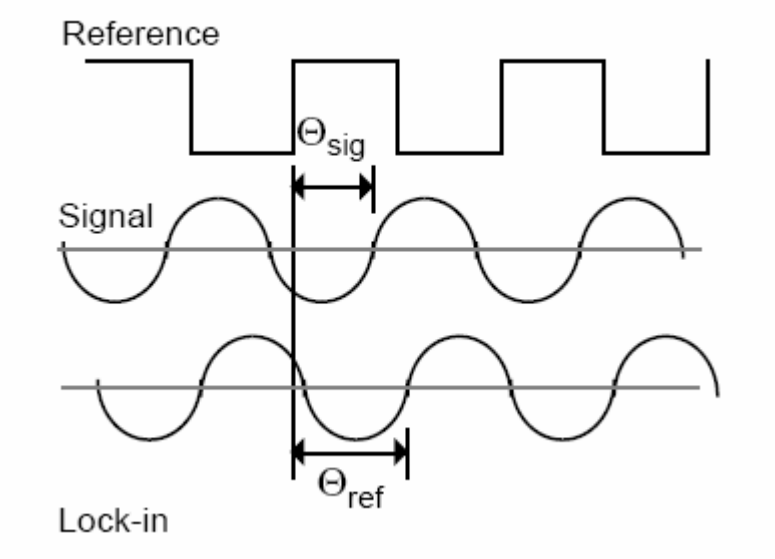

Figure 26. Output signal of the lock-in amplifier [31].

At the reference frequency a lock-in amplifier measures the single Fourier (sine) component of the signal, because of multiplying the signal and a pure sine wave. The input consists of signal and noise, where noise is interpreted as varying signals at all frequencies. In the ideal lock-in amplifier, noise at non reference frequencies is removed by the low pass filter, so lock-in provides "bandwidth narrowing". Only inputs at the reference frequency give an output [31].

6.2.2. **AC generator**

A signals generator TG215 (Thurlby Thandar Instruments) was used to feed the primary coil by electric current of the chosen frequency and amplitude. Frequency and amplitude were set manually on the front panel of the generator and they remain invariable during the measurements.

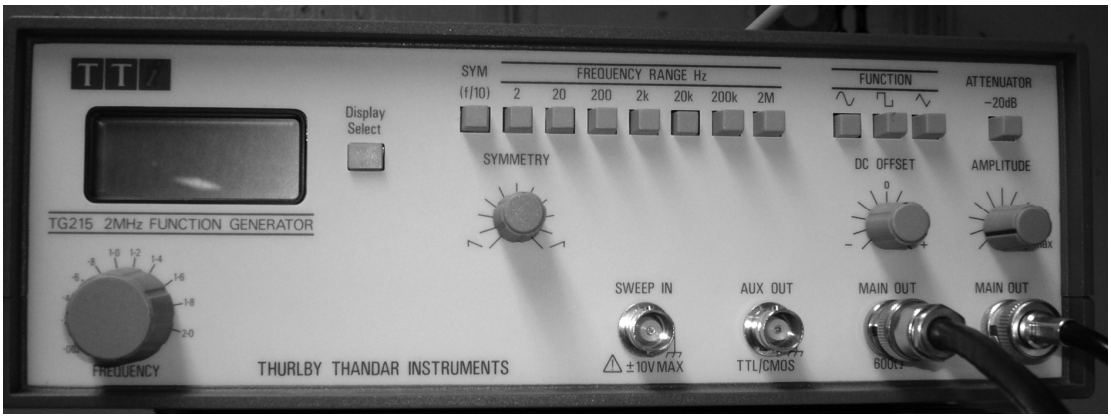

Figure 27. TG215 AC generator, front panel.

AC generator is one of the most universal test and measurement instrumentation available. It can generate waveshapes over a range of frequencies from mHz to MHz. From a low-impedance source a wide range of controlled constant amplitudes can be provided by the function generator. FM and AM modulation facilities can also be used.

Main functions [32]:

- 0.002 Hz to 2 MHz frequency range.
- Very high waveform quality at all frequencies & levels.
- 20 V peak to peak from 50 Ohms or 600 Ohms, plus TTL/CMOS output.
- 1000:1 frequency change by vernier or external voltage.
- Variable symmetry with constant frequency.

- Variable DC offset with zero detent.

- Digital display of frequency, amplitude and DC offset.

- Update rate at least 2 per second.

6.2.3. **Temperature controller**

Lake Shore 330 Autotuning Temperature Controller is used as a temperature controller in AC magnetometer.

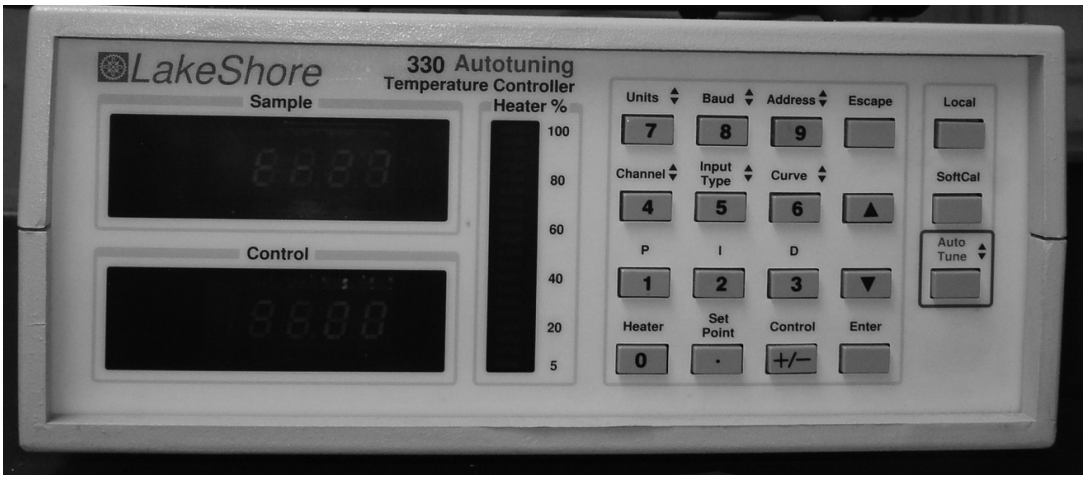

Figure 28. Lake Shore 330 autotuning temperature controller, front panel.

Temperature controller is a microprocessor-based device with digital control of a variable current output.

The Model 330 has two LED displays, which show data from both sensors, or from one sensor and the setpoint. There is also separate bar graph that displays heater output current. The Model 330 temperature controller is easy to operate because of the full function keypad.

The main properties of the Lake Shore 330 temperature controller are [33]:

1) Thermometry:

Number of Inputs: Two.

*Update Rate***:** Both Channels in 1 second.

Precision Curve Storage: Room for twenty 31-point Curves.

Thermocouples: Ch-AuFe (0.07 %), Ch-AuFe (0.03 %), Type E (Chromel-Constantan), Type K (Chromel-Alumel), and Type T (Copper-Constantan).

2) Control:

Control Type: Digital, three term PID with Autotuning.

Automatic Control Mode: P, PI, or PID control, user selectable.

Manual Control Mode: Gain (Proportional) 1 - 999, Reset (Integral) 1 - 999 sec., and Rate (Derivative) 0 – 200 % (0 - 500 sec.).

3) Computer Interfaces:

IEEE-488 Capabilities: Complies with IEEE-488.2 SH1, AH1, T5, L4, SR1, RL1, PP0, DC1, DT0, C0, E1.

Serial Interface: 300 or 1200 baud, RJ-11 connector (RS-232C electrical standard).

4) General:

Ambient Temperature Range: 20 to 30 °C (68 °F to 86 °F), or with reduced accuracy in range 15 °C to 35 °C (59 °F to 95 °F).

Power Requirements: 110, 120, 220, 240 VAC (+ 5 % - 10 %), 50 or 60 Hz; 135 W.

Two heater settings accommodate a variety of cryogenic systems and provide 25 W or 50 W maximum powers. The Model 330 power output is a quiet, variable DC current for as little noise coupling as possible between the heater and experiment. If lower power is required, two lower ranges are available with either of the settings [33].

6.2.4. **Stepper motor**

The unit, which provides the sample movement, is presented in Fig. 29.

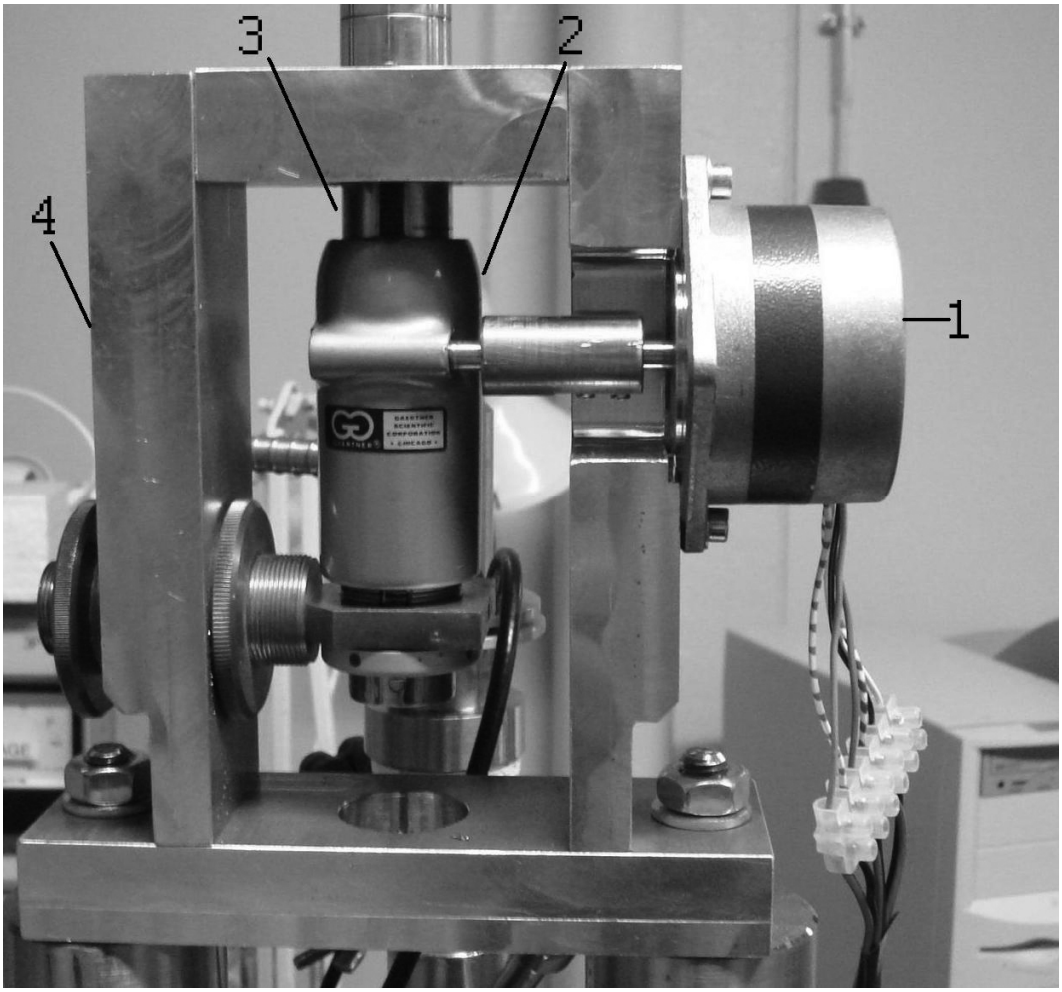

Figure 29. The sample driving unit. 1 is stepper motor, 2 is body of gear and the gear, 3 is the moving rack gear, and 4 is basement.

Stepper motors have the following benefits [34]:

• Low cost.

• Ruggedness.

• Simplicity in construction.

• High reliability.

• No maintenance.

• Wide acceptance.

• No tweaking to stabilize.

• No feedback components are needed.

• They work in just about any environment.

• High torque at low speeds.

• Inherently more failsafe than servo motors.

Stepper motor is a synchronous motor where the magnetic field is electronically switched to rotate the armature magnet around.

Stepper motors are electric motors without commutators. Stepper motors consist of a rotor and a stator. Rotating shaft with permanent magnet is the rotor [34] and the stator is electromagnets on the stationary portion that surrounds the motor. All of the commutation is controlled externally by the motor controller. The controllers and motors are designed so that the motor may be held in any fixed position as well as being rotated one way or the other. The repeatability and positioning depend on the geometry of the motor's rotor.

A stepping motor system consists of indexer, driver, and stepper motor, which is combined with some type of user interface (host computer or dumb terminal).

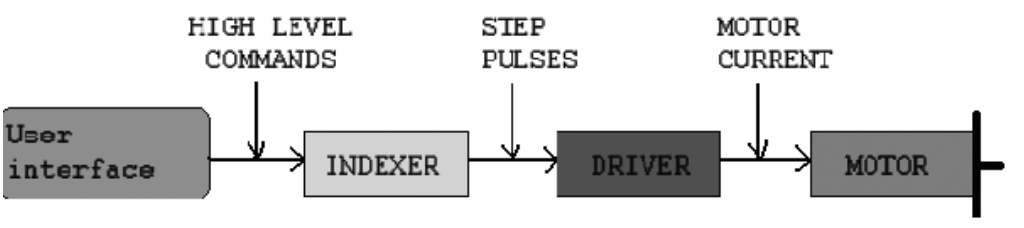

Figure 30. Ideology of the stepper motor system.

The indexer is also called a controller. It is a microprocessor capable to generate step pulses and direction signals for the driver. Typically, using the indexer avoids many other sophisticated command functions.

The driver (amplifier) converts the indexer command signals into the power necessary to feed the motor windings.

The stepper motor is an electromagnetic device that converts digital pulses into mechanical shaft rotation [35]. The resonance effect often exhibited at low speeds and decreasing torque with increasing speed are the main disadvantages in using a step motor.

In this kind of AC magnetometer was used the stepper motor 6500 – 15 - 4.1.6 SONCEBOZ SA. It is a hybrid unipolar stepper motor, which is constructed with multi-toothed stator poles and a permanent magnet rotor. This stepper motor has 200 rotor teeth and rotates at 1.80 step angles. The hybrid motor is shown in Fig. 31.

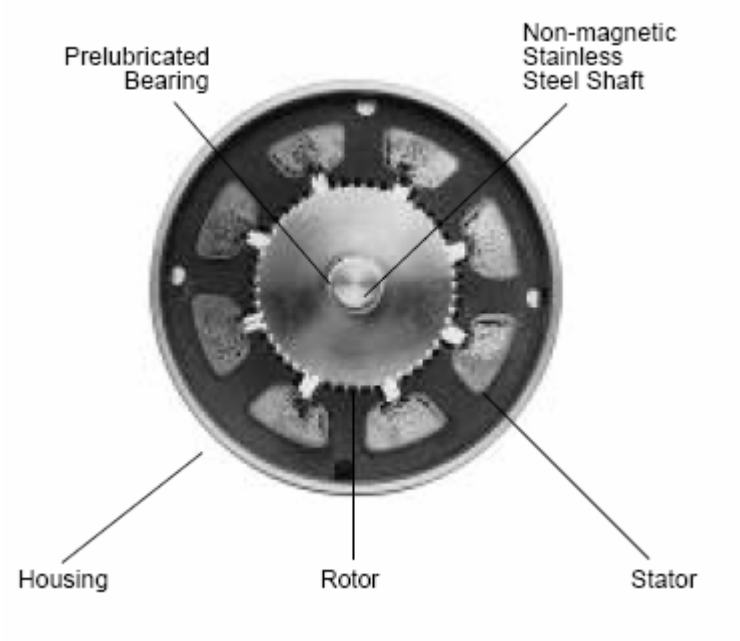

Figure 31. The hybrid motor.

6.2.5. **Control program**

Stepper motor, lock-in amplifier and temperature controller were controlled with a program developed based of LabVIEW.

The front panel of the program is presented in the Fig. 32.

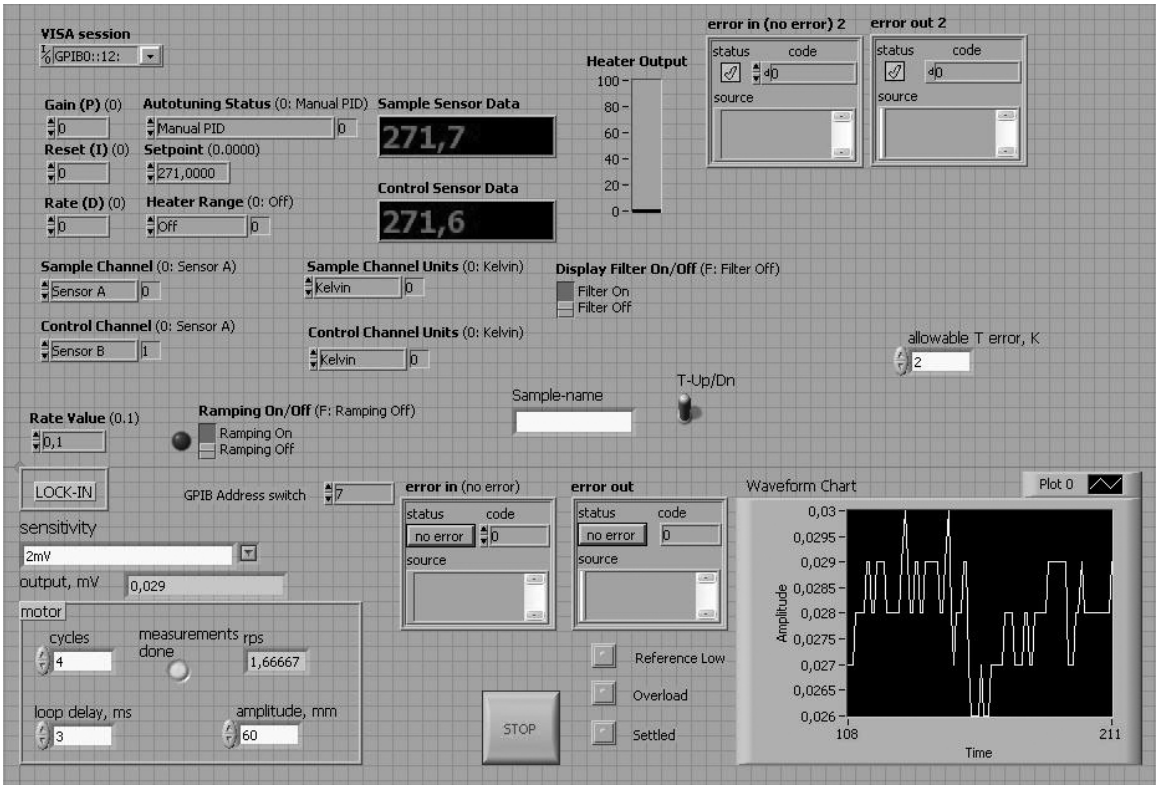

Figure 32. The front panel of the LabVIEW program.

Procedure of the program is the following. The user sets the “Setpoint” – value for the temperature of the sample, at which measurement will be carried out, “allowable T error, K”, which is the maximum deviation, and also the necessary parameters of stepper motor, lock-in amplifier and temperature controller.

When the program starts, read-in values from thermocouples appear in the fields “Sample Sensor Data” and “Control Sensor Data”. Average value of temperatures is calculated. This value is subtracted from the value set by the

user in the field “Setpoint”. The result is compared to a maximum deviation set in “allowable T error, K”, and if the difference is less than the limit, the stepper motor and the file recording of indications of the synchronous amplifier is simultaneously started.

7. Experimental results

The magnetic properties of $ZnGeP_2$:Mn were investigated in DC magnetic field with SQUID magnetometer and in AC magnetic field with AC magnetometer. Three $ZnGeP_2$:Mn samples were studied with Mn concentration c = 1.5 % mass, 3 % mass and 3.5 % mass.

7.1. Magnetic properties of $ZnGeP_2$:Mn in DC magnetic field

Samples of $ZnGeP_2$:Mn were measured in DC magnetic field using a SQUID magnetometer.

The measuring was done in following way. The sample was first cooled down to 3 K in zero magnetic field (zero field cooled, ZFC). Some time was given for the sample to reach thermal equilibrium before field was turned on. Then sample was heated in a magnetic field and in temperature range 3 K - 305 K the ZFC curve was obtained. After that, the sample was cooled down to 3 K in a magnetic field (field cooled case, FC). Finally, magnetic field was switched off and heating of magnetized sample started (thermoremanent residual magnetization, TRM).

Temperature dependencies of DC magnetization of $ZnGeP_2$:Mn with Mn concentration c = 3 % mass in different magnetic fields are shown in Figs. 33 - 41.

In Figs. 33 – 35 can be seen two distinct transitions at temperatures about 50 K and 300 K. At low temperatures $ZnGeP_2$:Mn with Mn concentration c = 3 % mass is in antiferromagnetic (AFM) state. Transition at T ~ 50 K can be identified as an antiferromagnetic (AFM) to ferromagnetic (FM) phase transition. Between T ~ 50 K and T ~ 300 K, this sample shows FM behavior. A FM to paramagnetic (PM) phase transition is seen at T ~ 300 K.

The T_c-value can be determined by the extrapolation of the steepest part of the *M(T)* curve until it crosses the *T*-axis [36].

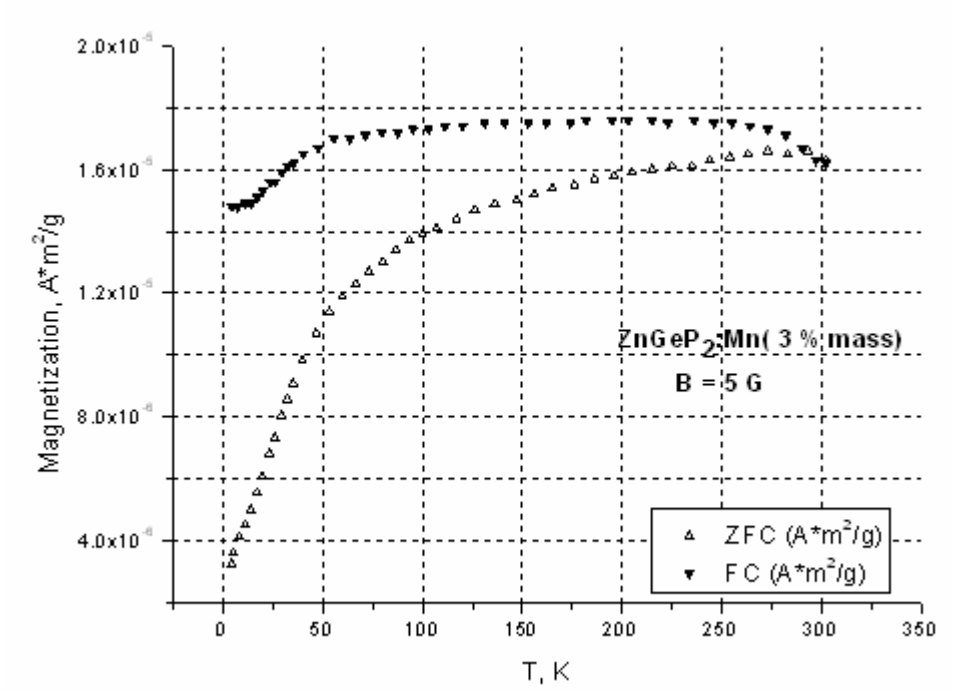

Figure 33. Temperature dependence of DC magnetization of $ZnGeP_2$:Mn (3 % mass) in magnetic field B = 5 G.

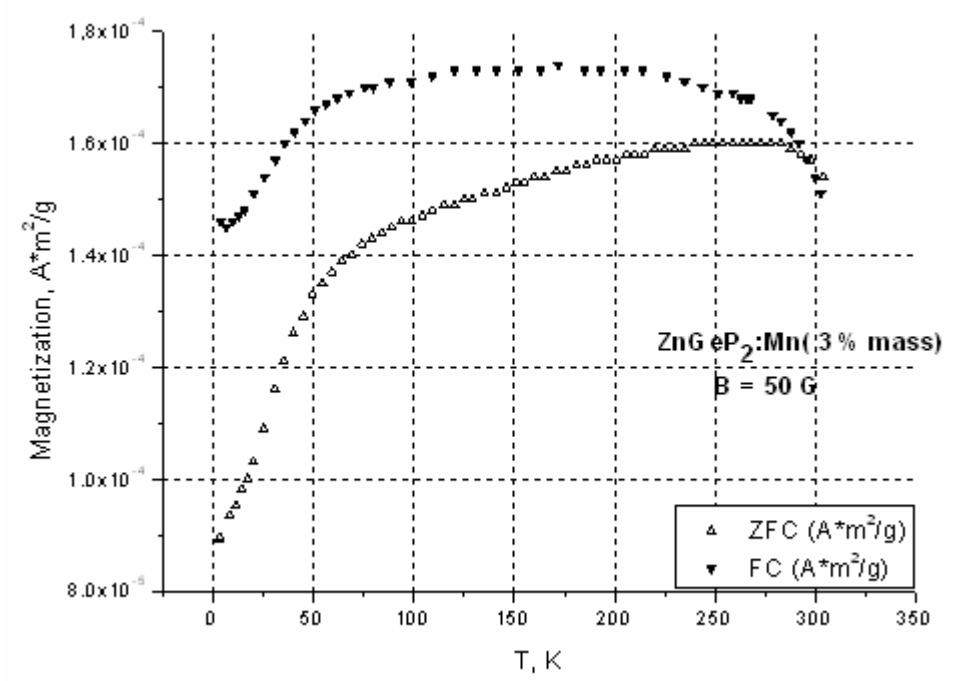

Figure 34. Temperature dependence of DC magnetization of $ZnGeP_2$:Mn (3 % mass) in magnetic field B = 50 G.

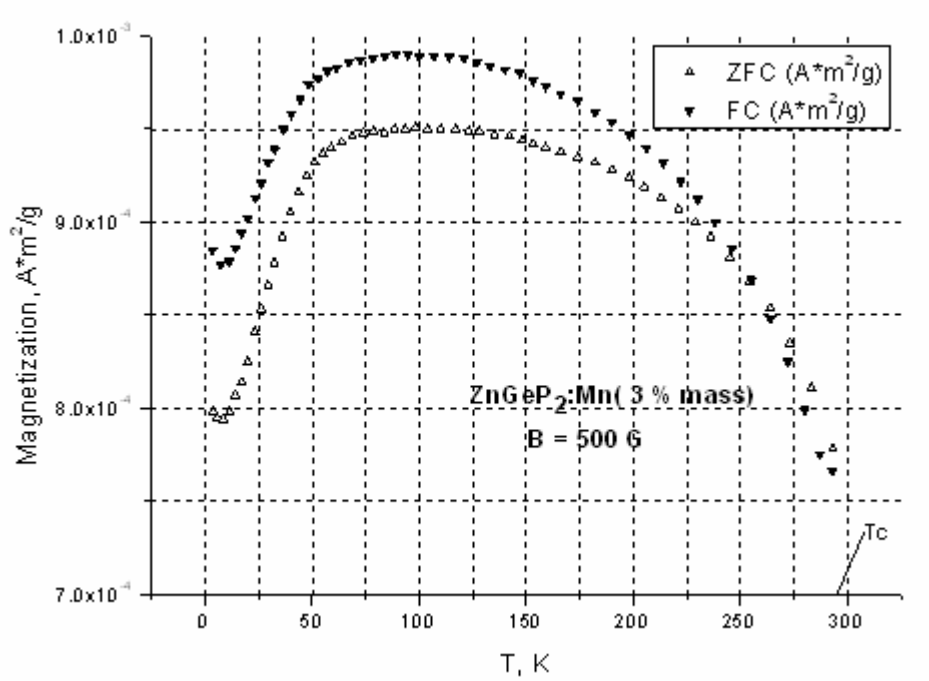

Figure 35. Temperature dependence of DC magnetization of $ZnGeP_2$:Mn (3 % mass) in magnetic field B = 500 G. T_c ~ 290 K.

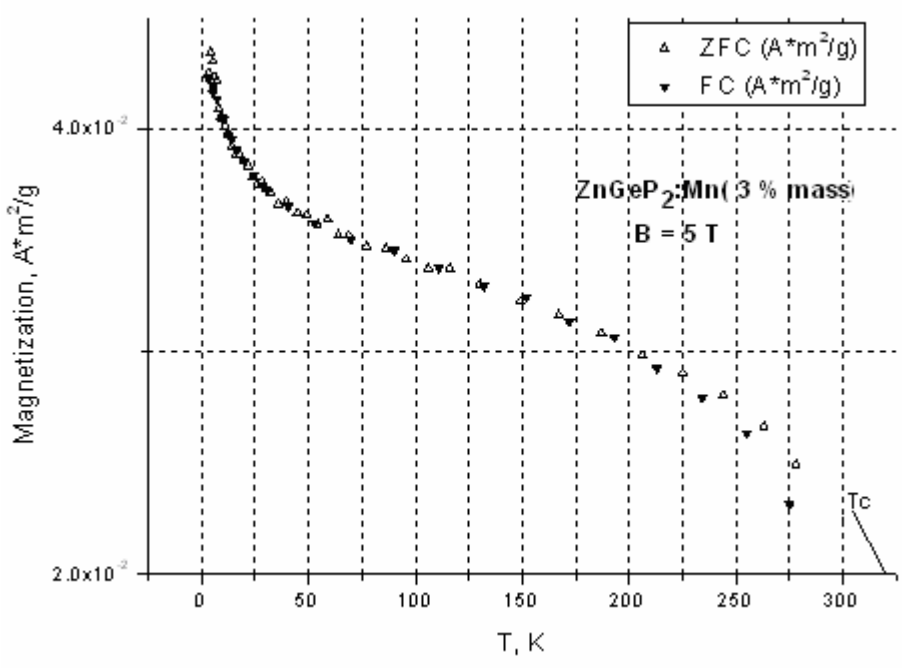

Figure 36. Temperature dependence of DC magnetization of $ZnGeP_2$:Mn (3 % mass) in magnetic field B = 5 T. T_c ~ 320 K.

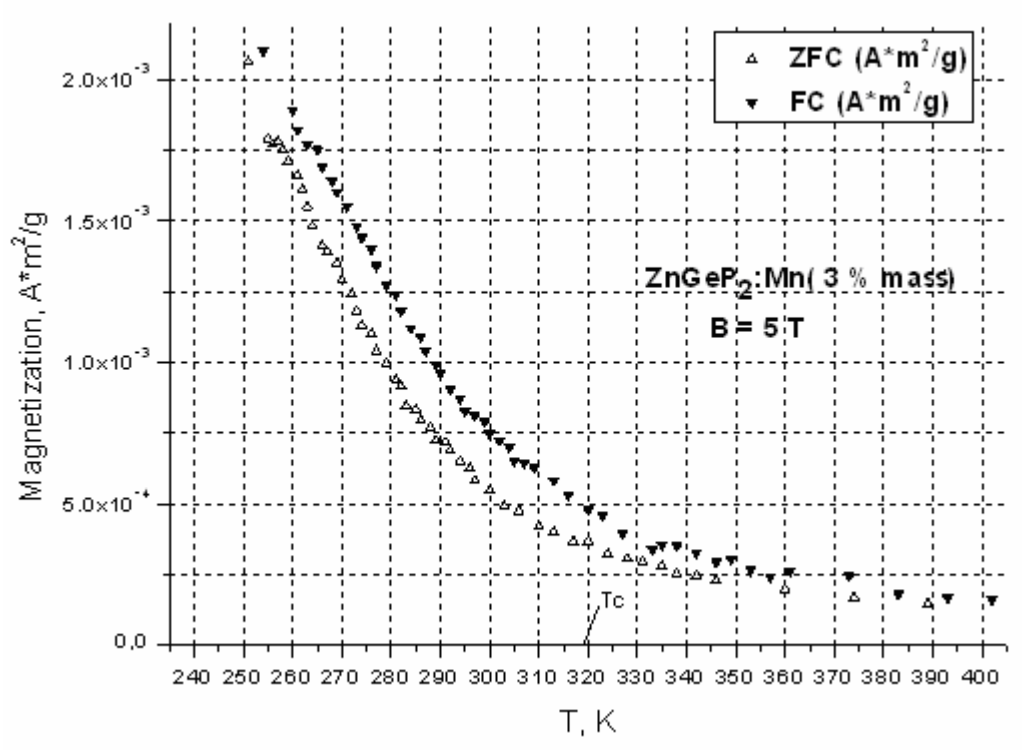

Figure 37. Temperature dependence of DC magnetization of $ZnGeP_2$:Mn (3 % mass) in magnetic field B = 5 T with enlarged scale and in high temperatures. T_c ~ 320 K.

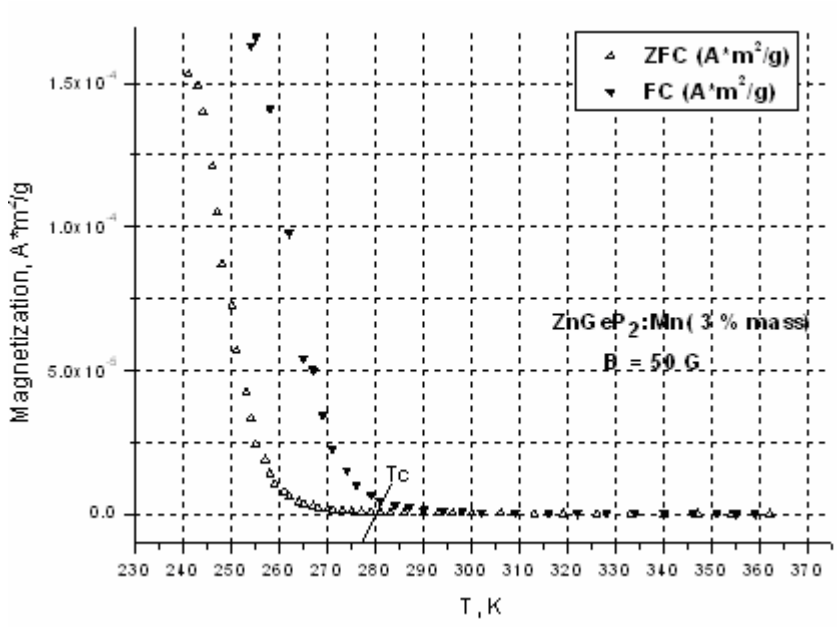

Figure 38. Temperature dependence of DC magnetization of $ZnGeP_2$:Mn (3 % mass) in magnetic field B = 50 G with enlarged scale and in high temperatures. T_c ~ 275 K.

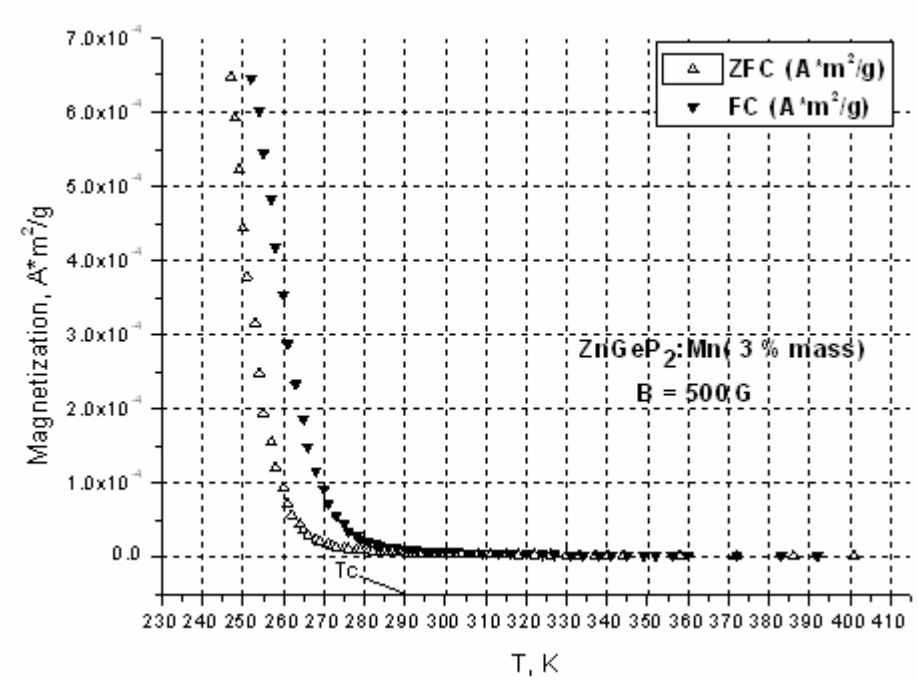

Figure 39. Temperature dependence of DC magnetization of $ZnGeP_2$:Mn (3 % mass) in magnetic field B = 500 G with enlarged scale and in high temperatures. T_c ~ 290 K.

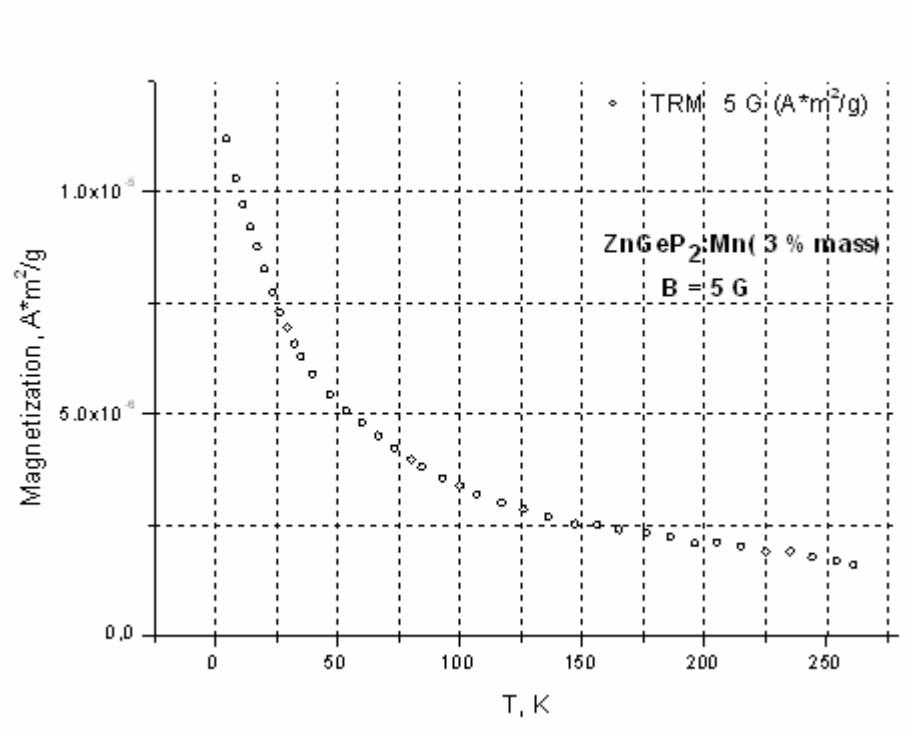

Figure 40. Temperature dependence of thermoremanent DC magnetization of $ZnGeP_2$:Mn (3 % mass) after field B = 5G.

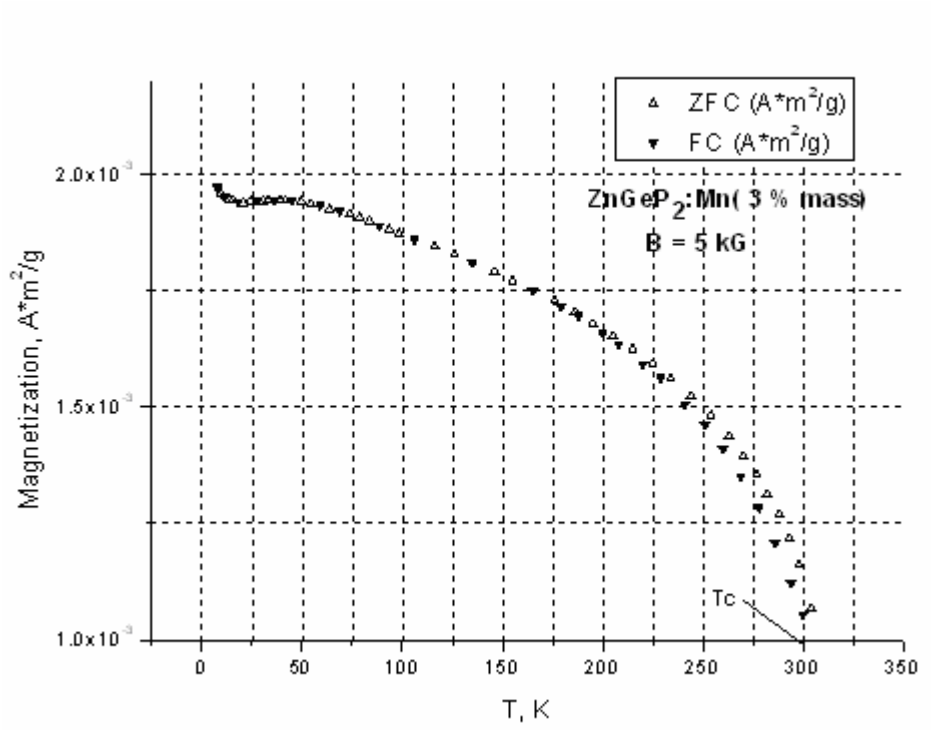

Figure 41. Temperature dependence of DC magnetization of $ZnGeP_2$:Mn (3 % mass) in magnetic field B = 5 kG. T_c ~ 300 K.

Temperature dependencies of DC magnetization of $ZnGeP_2$:Mn with the Mn concentration c = 1.5 % mass and 3.5 % mass in different magnetic field are shown in Figs. 42 – 45.

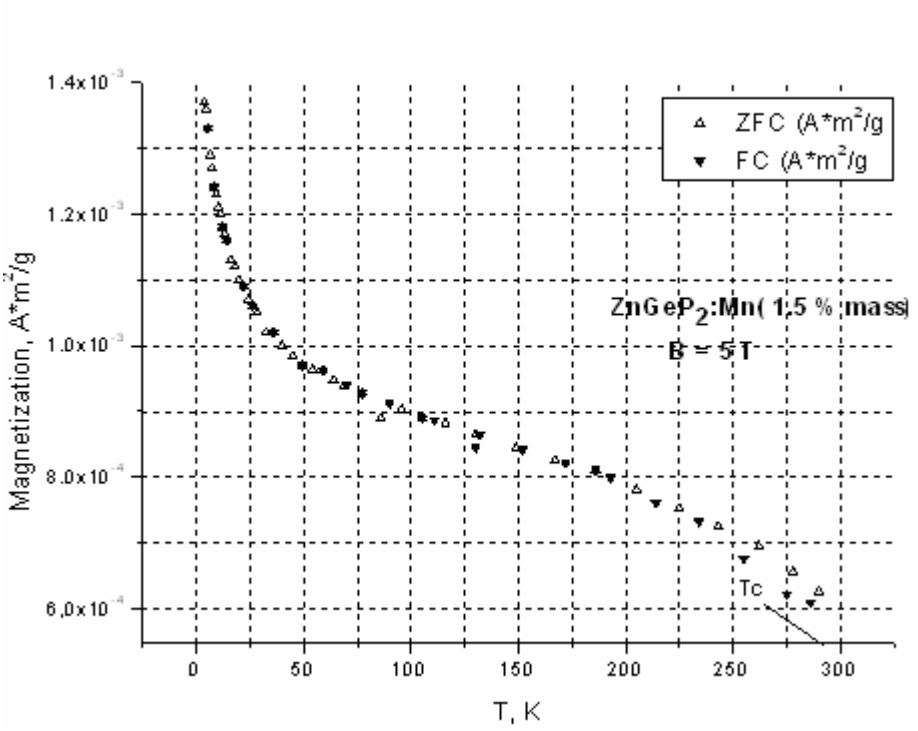

Figure 42. Temperature dependence of DC magnetization of $ZnGeP_2$:Mn (1.5 % mass) in magnetic field B = 5 T. T_c ~ 290 K.

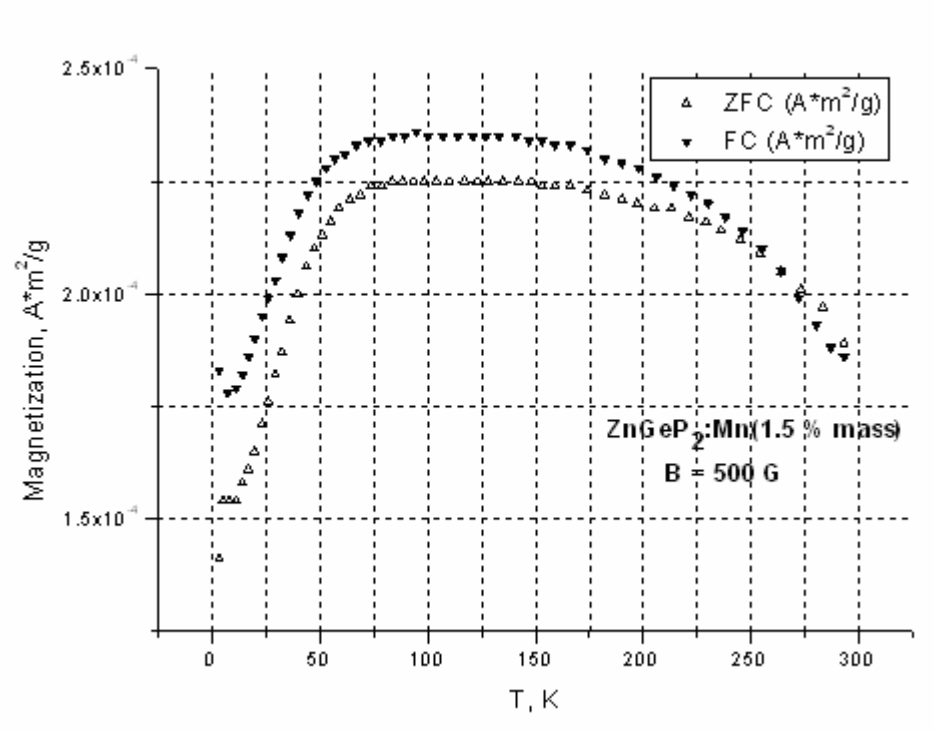

Figure 43. Temperature dependence of DC magnetization of $ZnGeP_2$:Mn (1.5 % mass) in magnetic field B = 500 G.

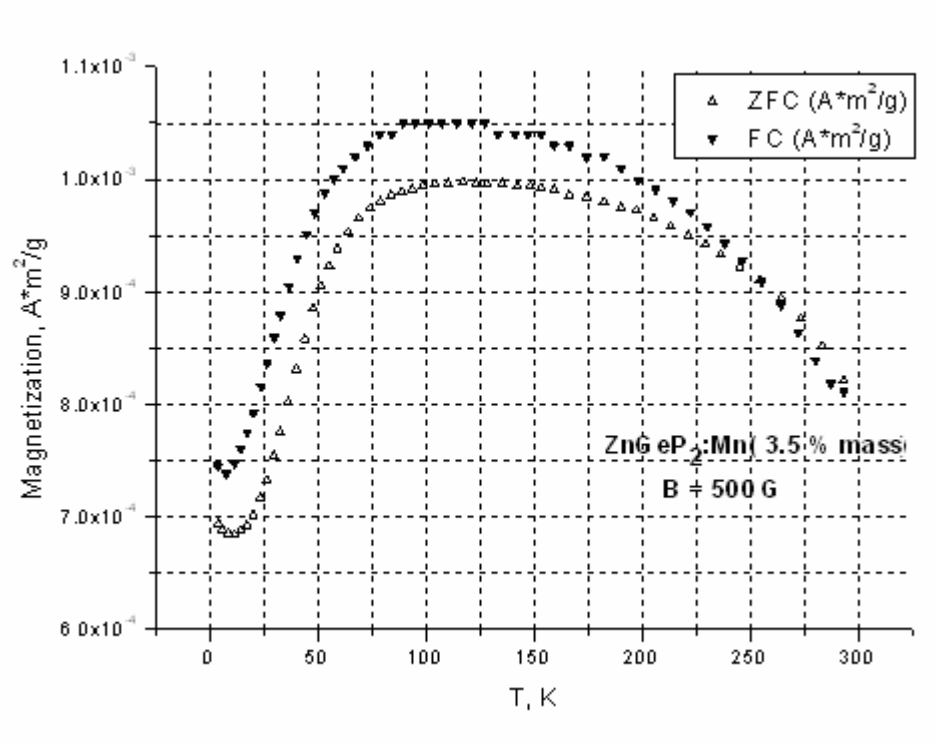

Figure 44. Temperature dependence of DC magnetization of $ZnGeP_2$:Mn (3.5 % mass) in magnetic field B = 500 G.

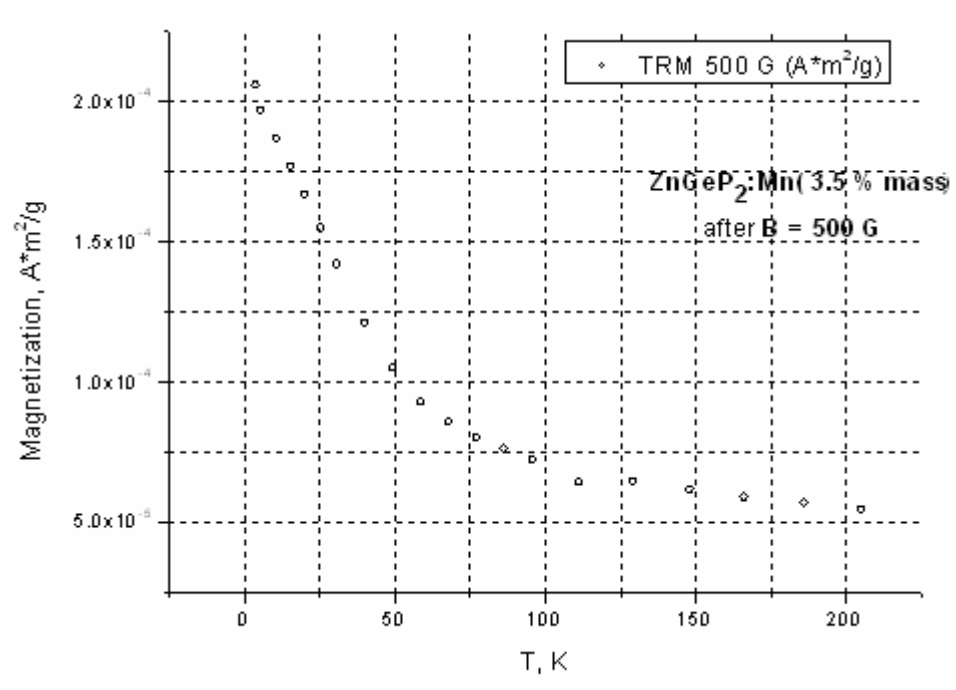

Figure 45. Temperature dependence of thermoremanent DC magnetization of $ZnGeP_2$:Mn (3.5 % mass) after field B = 500G.

Differences between ZFC and FC curves may be attributed to the existence of the Mn containing clusters.

Magnetic field dependence of $ZnGeP_2$:Mn (3 % mass) magnetization at 3 K, 50 K, 170 K and 300 K are presented in Figs. 47 - 50. *M(B)* dependencies for the $ZnGeP_2$:Mn samples obey the Langevin function.

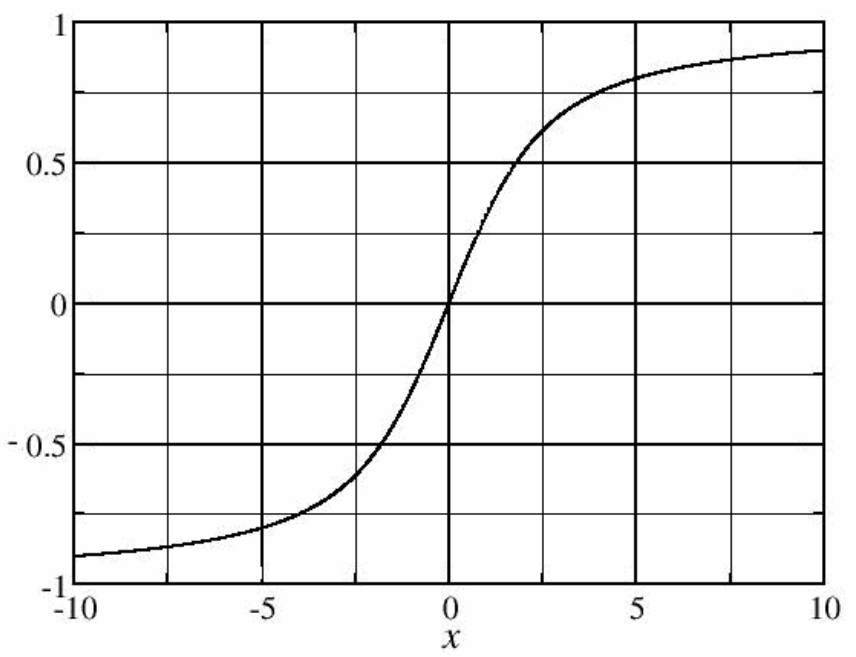

Figure 46. Langevin function.

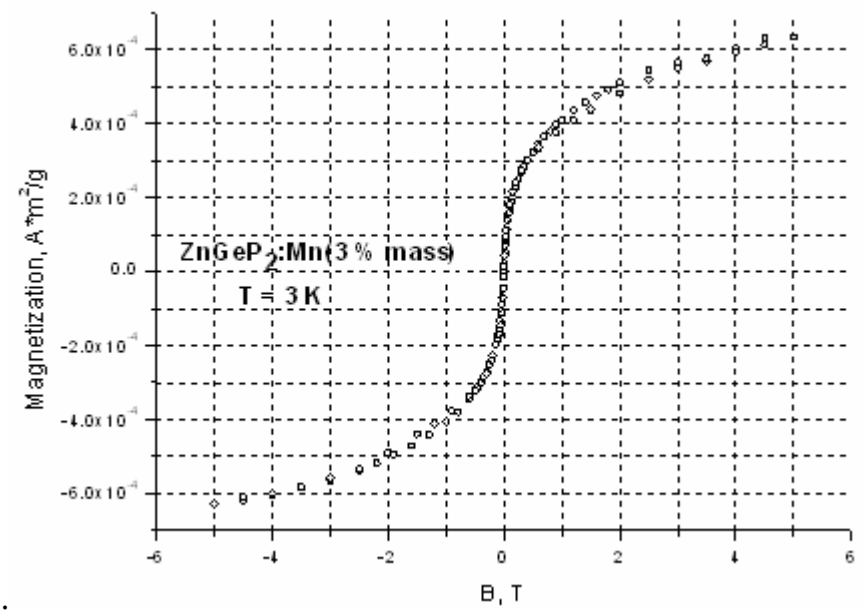

Figure 47. Magnetic field dependence of $ZnGeP_2$:Mn (3 % mass) magnetization at T = 3 K.

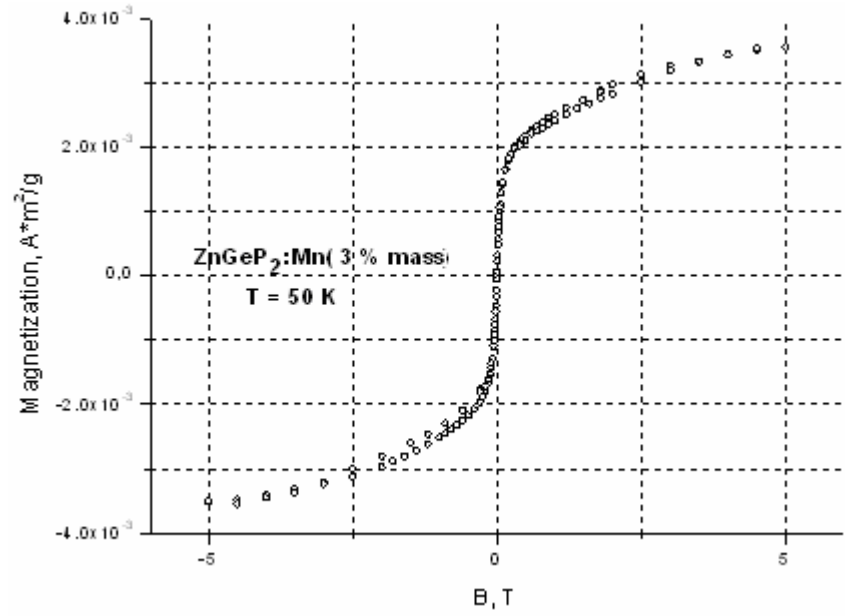

Figure 48. Magnetic field dependence of $ZnGeP_2$:Mn (3 % mass) magnetization at T = 50 K.

In Fig. 48 the saturation of $ZnGeP_2$:Mn (3 % mass) is seen in magnetic field B ≈ 0.2 T.

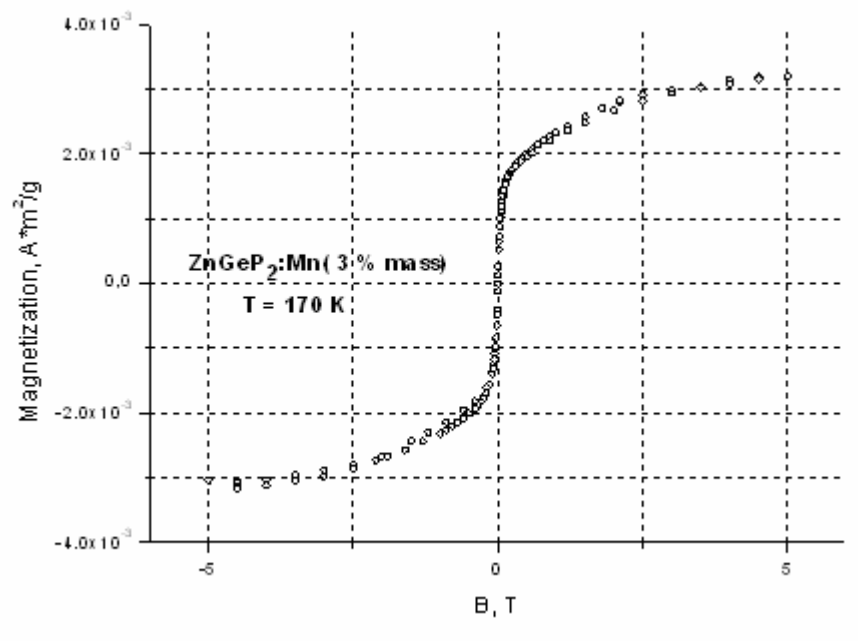

Figure 49. Magnetic field dependence of $ZnGeP_2$:Mn (3 % mass) magnetization at T = 170 K.

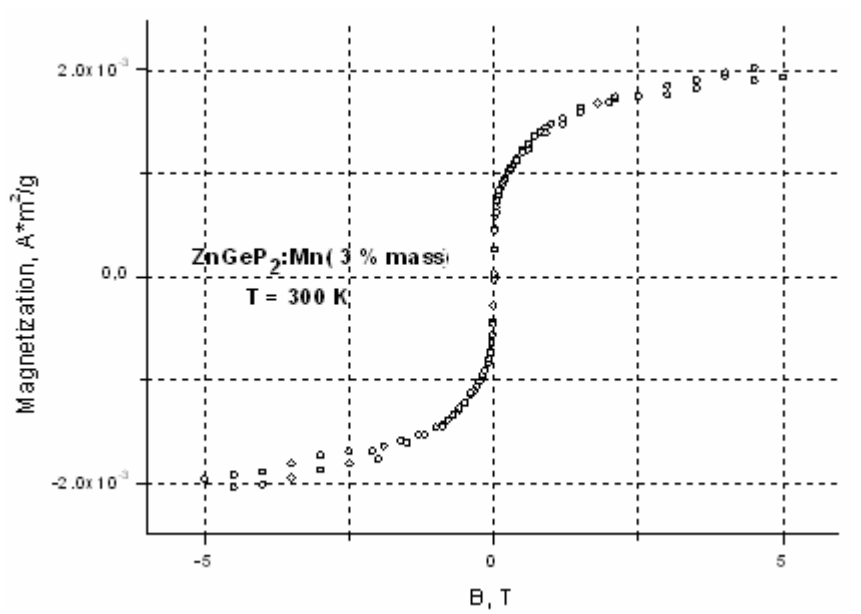

Figure 50. Magnetic field dependence of $ZnGeP_2$:Mn (3 % mass) magnetization at T = 300 K.

7.2. Magnetic properties of $ZnGeP_2$:Mn in AC magnetic field

To measure magnetization of the samples in different frequencies of AC magnetic field the AC magnetometer was used.

The results for $ZnGeP_2$:Mn sample with Mn concentration c = 3 % mass in magnetic field with different frequencies are shown in Figs. 51 - 52.

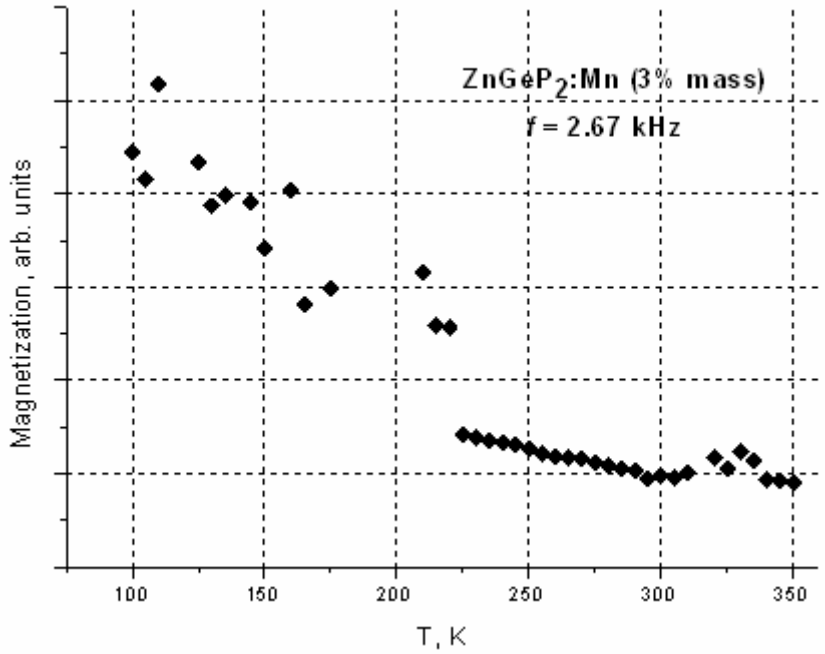

Figure 51. Temperature dependence of AC magnetization of $ZnGeP_2$:Mn (3 % mass) in AC magnetic field with frequency f = 2.67 kHz.

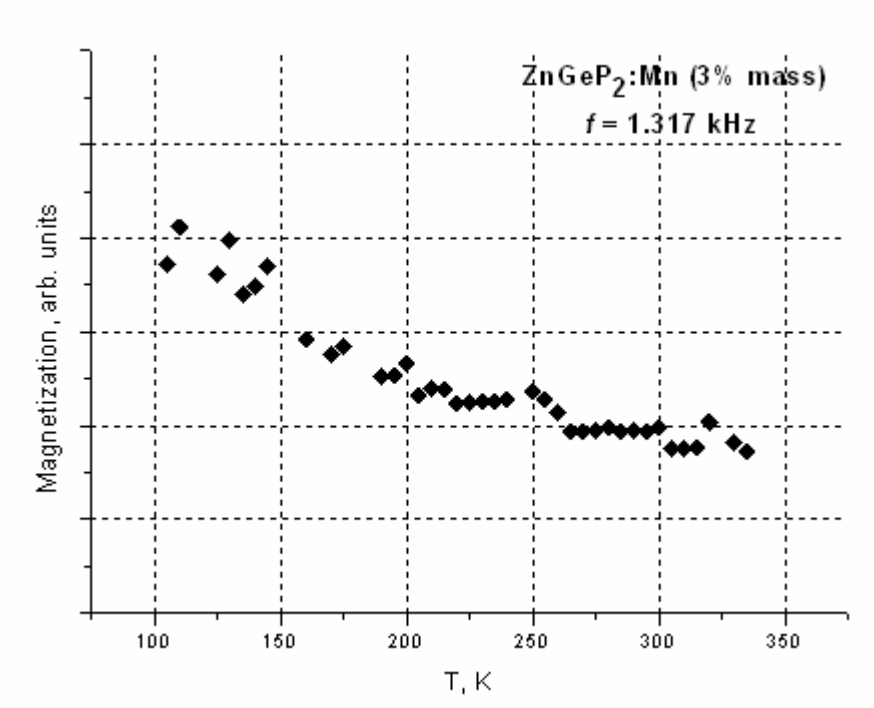

Figure 52. Temperature dependence of AC magnetization of $ZnGeP_2$:Mn (3 % mass) in AC magnetic field with frequency f = 1.317 kHz.

In Fig. 53 are shown the results for $ZnGeP_2$:Mn sample with Mn concentration c = 3.5 % mass.

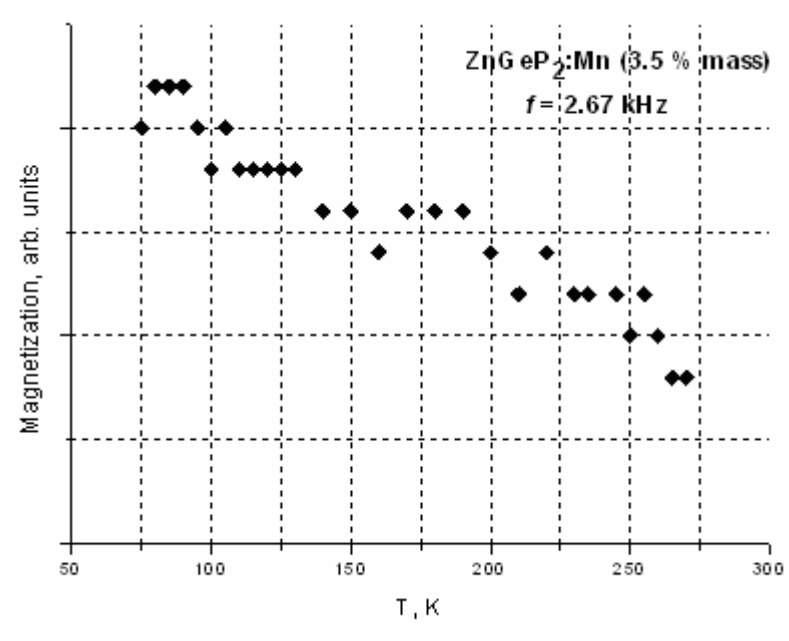

Figure 53. Temperature dependence of AC magnetization of $ZnGeP_2$:Mn (3.5 % mass) in AC magnetic field with frequency f = 2.67 kHz.

The results for $ZnGeP_2$:Mn sample with Mn concentration c = 1.5 % mass are shown in Figs. 54 - 55.

The sensitivity and digital levels of the AC magnetometer is clearly seen in Fig. 55. Also in this figure a sharp slope is seen. This slop is very similar to the slope in Fig. 43.

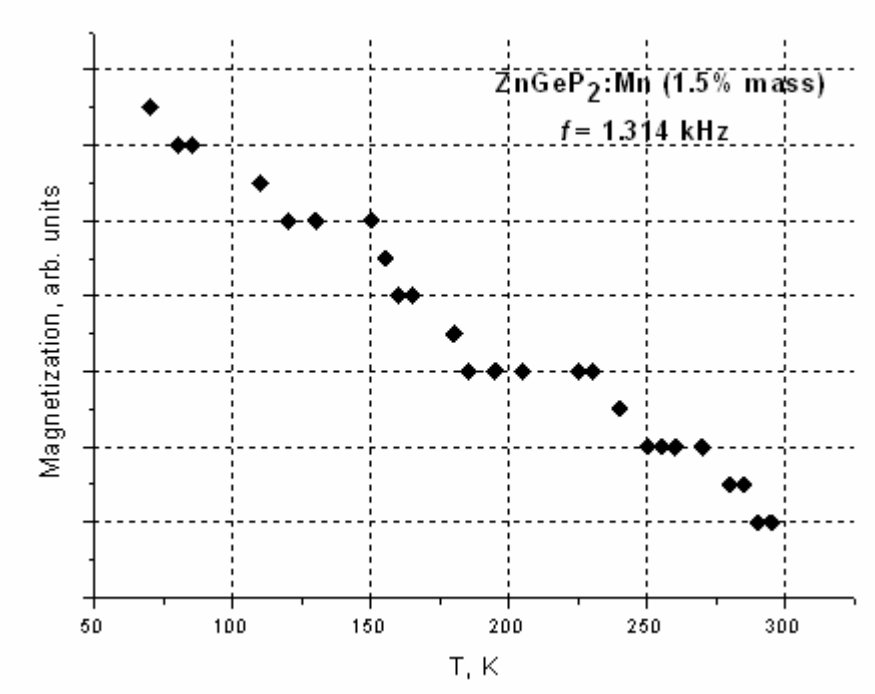

Figure 54. Temperature dependence of AC magnetization of $ZnGeP_2$:Mn (1.5 % mass) in magnetic field with frequency f = 1.314 kHz.

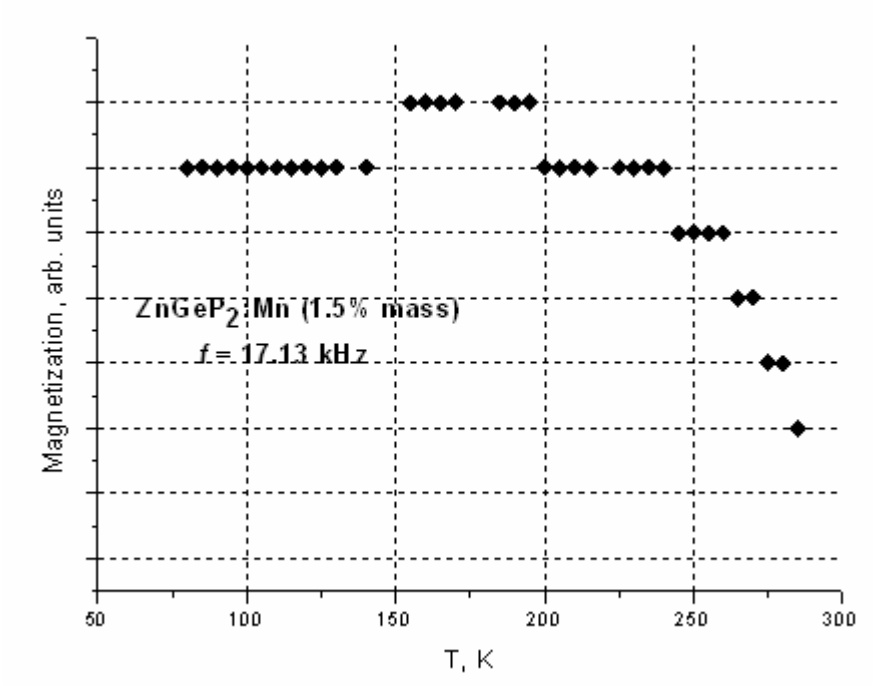

Figure 55. Temperature dependence of AC magnetization of $ZnGeP_2$:Mn (1.5 % mass) in magnetic field with frequency f = 17.13 kHz.

8. Comparison of the results of AC and DC magnetometry

The superposition of *M(T)* dependencies obtained in AC and DC magnetic fields are presented in Figs. 56 - 57.

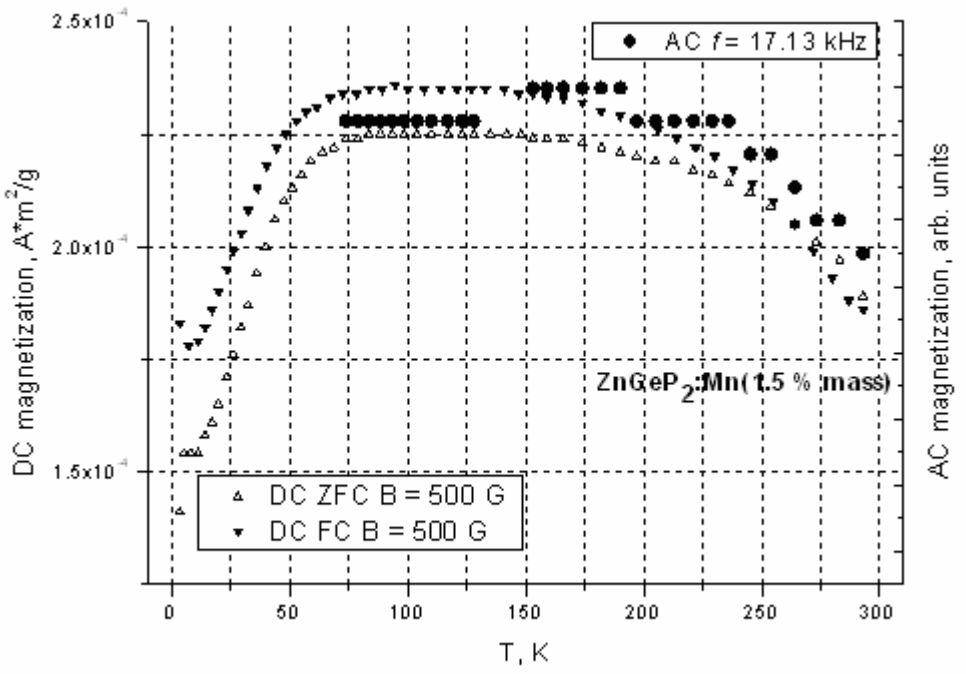

Figure 56. Temperature dependencies of AC and DC magnetization for $ZnGeP_2$:Mn (1.5 % mass).

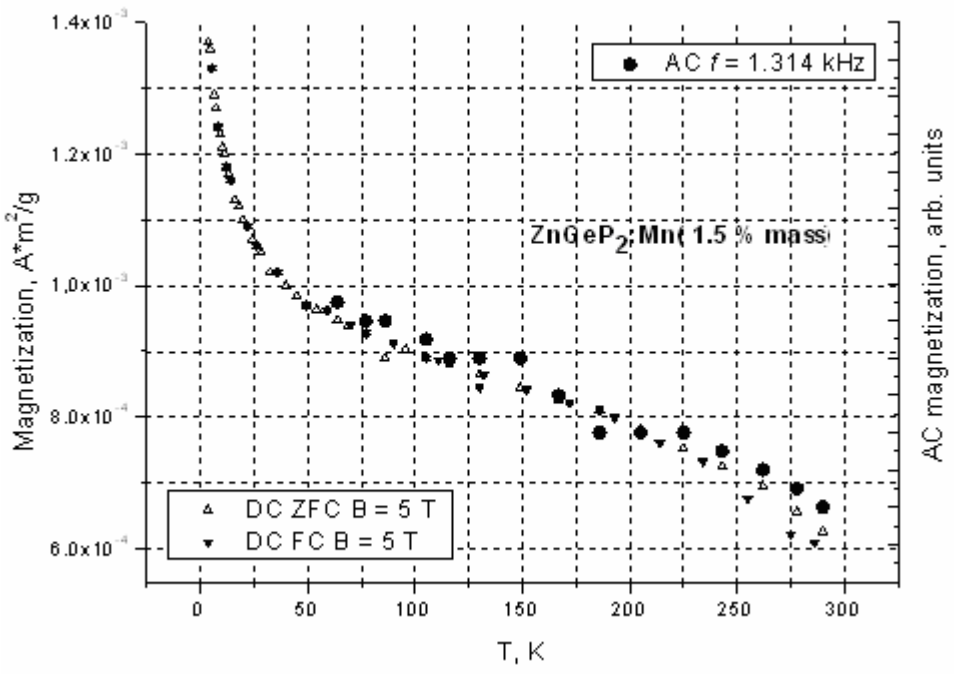

Figure 57. Temperature dependencies of AC and DC magnetization for $ZnGeP_2$:Mn (1.5 % mass).

In Figs. 56 and 57 is clearly seen the agreement between the results obtained in AC and DC magnetometers.

9. Processing of experimental data

The results, which were obtained in AC magnetometer, are not so perfect in comparison with DC magnetometer results because of the small magnetization value of the samples.

Using Origin 8, the program for professional data analysis, the computer processing of the AC magnetometer results was obtained (Figs. 58 - 62).

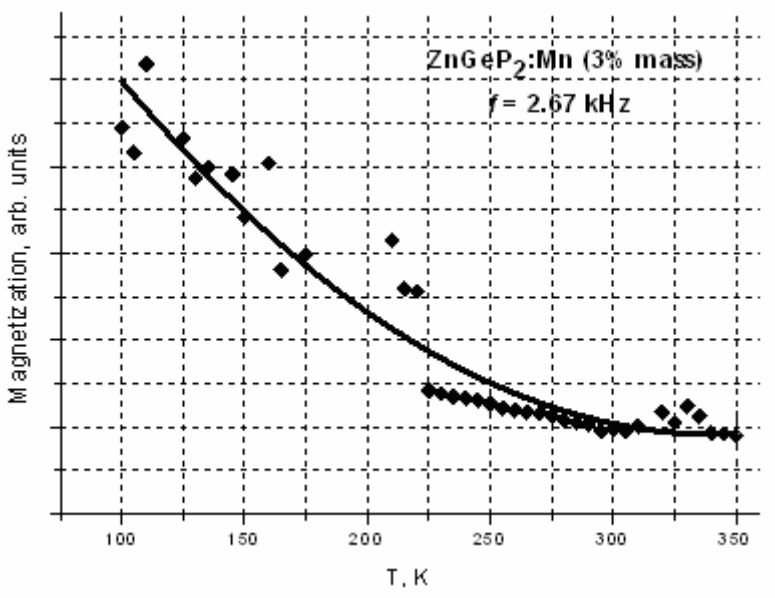

Figure 58. Temperature dependence of AC magnetization of $ZnGeP_2$:Mn (3 % mass) in magnetic field with frequency f = 2.67 kHz after polynomial fitting, using Origin 8, with polynomial order = 2.

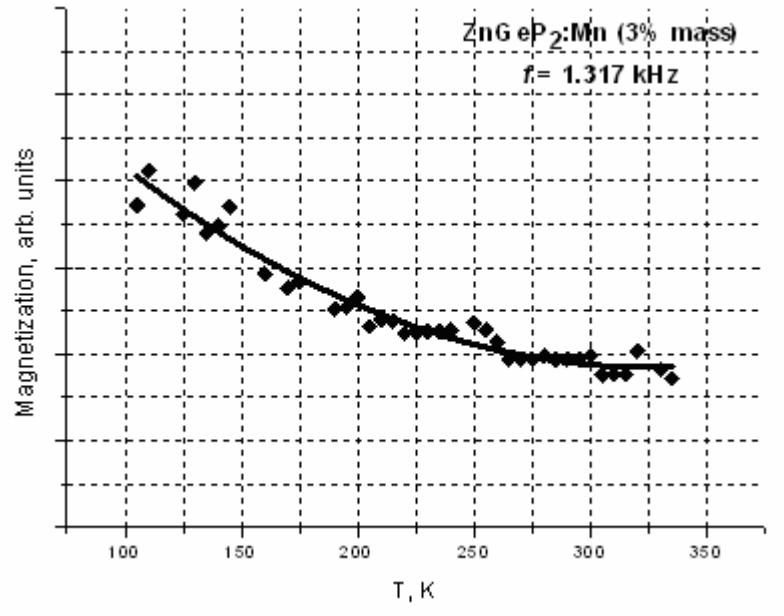

Figure 59. Temperature dependence of AC magnetization of $ZnGeP_2$:Mn (3 % mass) in magnetic field with frequency f = 1.317 kHz after polynomial fitting, using Origin 8, with polynomial order = 2.

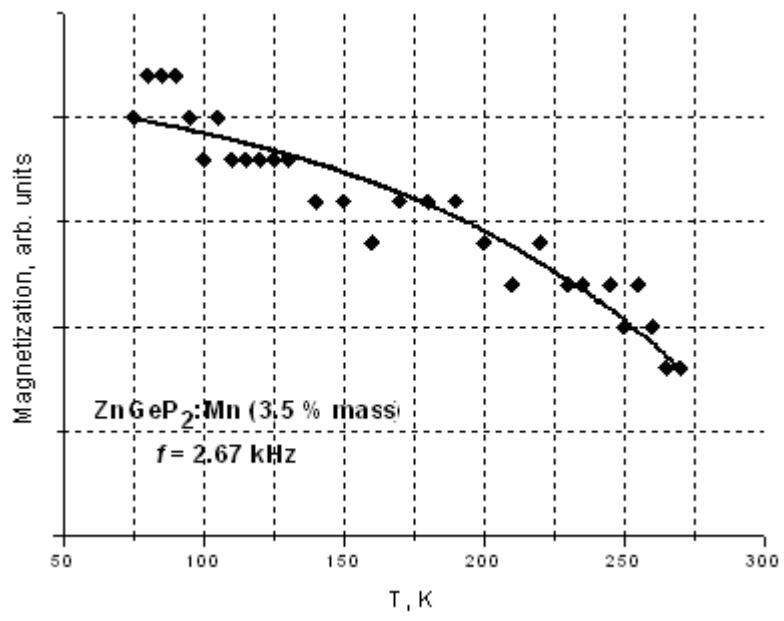

Figure 60. Temperature dependence of AC magnetization of $ZnGeP_2$:Mn (3.5 % mass) in magnetic field with frequency f = 2.67 kHz after exponential fitting, using Origin 8, with formula:

$$y = y_0 + Ae^{-x/t}. \tag{10}$$

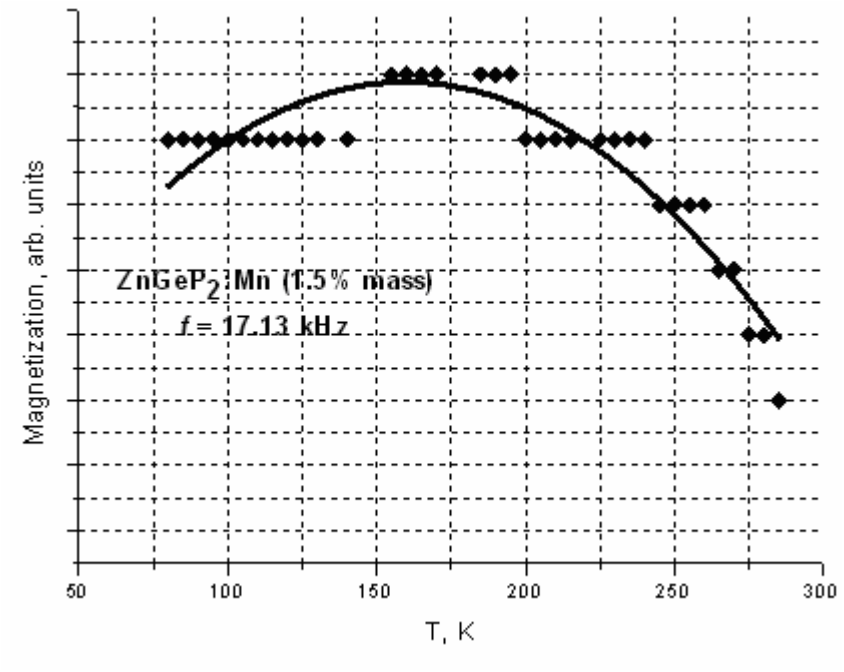

Figure 61. Temperature dependence of AC magnetization of $ZnGeP_2$:Mn (1.5 % mass) in magnetic field with frequency f = 17.13 kHz after polynomial fitting, using Origin 8, with polynomial order = 2.

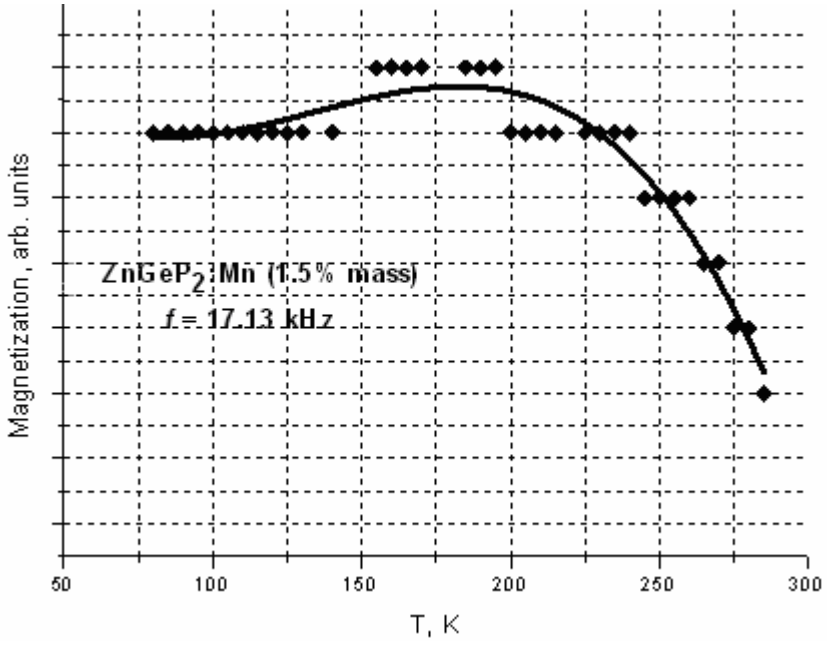

Figure 62. Temperature dependence of AC magnetization of $ZnGeP_2$:Mn (1,5 % mass) in magnetic field with frequency f = 17.13 kHz after cubic polynomial fitting, using Origin 8, with formula:

$$y = A + Bx + Cx^2 + Dx^3. \qquad (11)$$

10. Conclusions

In this work is presented a review of magnetic properties of materials, different kinds of magnetic material, and results of magnetic measurements.

Magnetic properties of $ZnGeP_2$:Mn were investigated in DC magnetic field up to B = 5 T in the temperature range from 3 K up to 400 K (SQUID) and in AC magnetic field in the temperature range from 77 K up to 350 K in frequency range from 500 Hz up to 18 KHz (AC magnetometer). The *M(H)* and *M(T)* dependencies were obtained and presented

At low temperatures $ZnGeP_2$:Mn with Mn concentration c = 3 % mass is in antiferromagnetic state. Transition at T ~ 50 K can be identified as an antiferromagnetic to ferromagnetic phase transition. Between T ~ 50 K and T ~ 300 K, this sample shows FM behavior. A ferromagnetic to paramagnetic phase transition is seen at T_c ~ 300 K.

Also difference between ZFC and FC curves was detected, which is clear spin glass behavior.

Confirmation of AC measurements by DC measurements in $ZnGeP_2$:Mn sample with Mn concentration c = 1.5 % mass were carried out. Also smoothing of experimental points obtained in AC measurements is presented in this work.

It is necessary to continue work with this material, start to grow thin films and explore their properties.

11. References

[1] D. Jiles, Introduction to Magnetism and Magnetic Materials, Chapman and Hall, 1991.

[2] B.D. Cullity, Introduction to Magnetic Materials, Addison-Wesley, 1972.

[3] S.V. Vonsovsky, Magnetism. Moscow: Nauka, 1971 (in Russian).

[4] V.P. Karsev, Magnet for the three thousand years. Moscow, 1972 (in Russian).

[5] McGraw-Hill, Concise Encyclopedia of Physics. The McGraw-Hill Companies, Inc., 2002.

[6] D.D. Mishin, Magnetic material. Moscow, 1981 (in Russian).

[7] A.I. Ashiezer, General physics, Electrical and magnetic phenomena. Kiev, 1981 (in Russian).

[8] A.N. Matveev, Electricity and magnetism, Moscow: Vyshaya schkola, 1983 (in Russian).

[9] E.V. Kyzmin, T. A. Petrakovsky, Physics of the magnetic order matter. Novosibirsk: Nayka, 1976(in Russian).

[10] T. A. Petrakovsky, Amorphous magnetics. Novosibirsk, 1981 (in Russian).

[11] I. Korenblit, E. F. Shender, Spin glasses. Mockow: Znanie, 1984 (in Russian).

[12] Cannella V., Mydosh J., Magnetic Ordering in Gold - Iron Alloys, Phys. Rev. B. 1972. Vol. 6. P. 4220 - 4237.

[13] Sherrington D., Kirkpatrick S., Solvable Model of a Spin-Glass, Phys. Rev. Letters. 1975. Vol. 35. P. 1792 - 1795.

[14] Edwards S.F., Anderson P.W. Short-Range Ising Model of Spin Glasses, J. Phys. F. 1975. Vol. 5. P. 965 - 974.

[15] G.A. Prinz, Science 250, 1990.

[16] M. I. Dyakonov, in Future Trends in Microelectronics: TheNano, the Giga, and the Ultra. IEEE Press, New York, 2004.

[17] V. Yu. Rud' and Yu.V. Rud', Tech. Phys. Lett. 23, 415, 1997.

[18] S. Cho, S. Choi, G. Cha, S.C. Hong, Room-Temperature Ferromagnetism in $(Zn_{1-x}Mn_x)GeP_2$ Semiconductors, Phys. Rev. Lett. 88, 2002.

[19] G. C. Bhar, S. Das, U. Chatterjee, and K. L. Vodopyanov, Appl. Phys. Lett. 54, 313, 1989.

[20] S. Limpijumnong, W. Lambrecht, B. Segall, Electronic structure of $ZnGeP_2$: A detailed study of the band structure near the fundamental gap and its associated parameters.,Phys. Rev. Lett. 60, 11, 8087-8096, 1999.

[21] Bridgman Method, Accessed 10 March 2009, www.mtixtl.com/xtlflyers/bridgman.doc.

[22] S. G. Taranov , N.E. Fevrleva, Magnetic measurements. Moscow, 1984 (in Russian).

[23] Yu. Maslov Magnetic measurements and devices. Vladimir: Vladimir, 1982 (in Russian).

[24] Yu. Seleznev, Metods and structure of the magnetics and electrical measurements.Omsk, 1987(in Russian).

[25] I.V. Savel'ev, General physics, №2. Fizmatgiz, 1978 (in Russian).

[26] M. McElfresh, Fundamentals of Magnetism and Magnetic Measurements, Quantum Design, 1994.

[27] I.A. Alfaleh, M. Shahabuddin and N. S. Alzayed, Low cost AC susceptometer using closed cycle helium cryostat, 2002.

[28] J. Park, E. Vescovo, H. Kim, C. Kwon, R. Ramesh, T. Venkatesan. Phys. Rev. Lett., 1998.

[29] K. J. Thomas, Antiferromagnetism, ferromagnetism and magnetic phase separation in $Bi_2Sr_2CoO_{6+\delta}$, Massachusetts Institute of Technology, 2003.

[30] GPIB Controller for Hi-Speed USB, Accessed 20 March 2009, http://www.ni.com/pdf/products/us/20055194101101dlr.pdf.

[31] What is a lock-in amplifier? Accessed 25 March 2009, http://www.signalrecovery.com.

[32] Thurlby Thandar Instruments. TG200 Series. User manual.

[33] Model 330 autotuning temperature controller user's manual.

[34] How Stepper Motors Work. Accessed 2 April 2009, http://www.imagesco.com/articles/picstepper/02.html.

[35] Stepper Motor System Basics, Accessed 2 April 2009, http://www.ams2000.com/stepping101.html.

[36] S. Choi, G.-B. Cha, S.C. Hong, S. Cho, Y. Kim, J.B. Ketterson, S.-Y. Jeong, G.-C. Yi, Solid State Commun, 122, 2002.